HHS Public Access

Author manuscript

*Sci Immunol*. Author manuscript; available in PMC 2022 November 30.

Published in final edited form as:

*Sci Immunol*. 2022 May 06; 7(71): eabf3717. doi:10.1126/sciimmunol.abf3717.

# Zbtb20 identifies and controls a thymus derived population of regulatory T cells that play a role in intestinal homeostasis

**Agata K. Krzyzanowska**[1,3], **Rashade A.H. Haynes II**[1,7], **Damian Kovalovsky**[4], **Hsinching Lin**[1], **Louis Osorio**[1], **Karen L. Edelblum**[5], **Lynn M. Corcoran**[6], **Arnold B. Rabson**[1,2,3], **Lisa K. Denzin**[1,2,3], **Derek B. Sant'Angelo**[1,2,3,*]

[1]Child Health Institute of New Jersey, Rutgers Robert Wood Johnson Medical School, New Brunswick, NJ 08901, USA

[2]Department of Pediatrics and Pharmacology, Rutgers Robert Wood Johnson Medical School, New Brunswick, NJ 08901, USA

[3]Rutgers Graduate School of Biomedical Sciences, Rutgers Robert Wood Johnson Medical School, New Brunswick, NJ 08901, USA

[4]Center for Cancer Research National Cancer Institute, National Institute of Health, Bethesda, MD 20892, USA

[5]Department of Pathology & Laboratory Medicine, Center for Immunity and Inflammation, Rutgers New Jersey Medical School, Newark, NJ 07103

[6]The Walter and Eliza Hall Institute of Medical Research, Immunology Division, Department of Medical Biology, The University of Melbourne, Parkville, Victoria 3052, Australia

[7]Current affiliation: Immuno- and Molecular Toxicology, Nonclinical Research and Development Bristolm Myers Squibb, 1 Squibb Dr, New Brunswick, NJ 08903

## Abstract

The expression of BTB-ZF transcription factors such as ThPOK in $CD4^+$ T cells, Bcl6 in T follicular helper cells, and PLZF in natural killer T cells defines the fundamental nature and characteristics of these cells. Screening for lineage-defining BTB-ZF genes led to the discovery of a subset of T cells that expressed Zbtb20. Approximately half of $Zbtb20^+$ T cells expressed FoxP3, the lineage-defining transcription factor for regulatory T cells (Tregs). $Zbtb20^+$ Tregs were phenotypically and genetically distinct from the larger conventional Treg population. $Zbtb20^+$ Tregs constitutively expressed mRNA for IL-10 and produced high levels of the cytokine upon

[*]Corresponding author: Derek B. Sant'Angelo, Child Health Institute of New Jersey, Rutgers Robert Wood Johnson Medical School, 89 French St. New Brunswick, NJ 08901, 732-235-9394, santandb@rwjms.rutgers.edu.

Author contributions

A.K.K, R.A.H.H., D.K., L.K.D., and D.B.S. conceived the overall project and designed the experimental plan. A.K.K., R.A.H.H., D.K., and H.L. planned and carried out experiments. L.M.C. generated the $Zbtb20^{flox/flox}$ mice and monoclonal antibodies. A.B.R. performed histological imaging of the mouse colons. H.L. carried out ChIP experiments. L.O. assisted with mouse work. Data were discussed and interpreted by A.K.K., R.A.H.H., D.K., K.L.E., H.L. A.B.R., L.K.D, and D.B.S. The manuscript was written by A.K.K. and D.B.S. and critically reviewed by L.K.D, R.A.H.H., D.K., L.M.C, K.L.E., and A.B.R.

Competing interests.

Derek B. Sant'Angelo, Agata Krzyzanowska and Lisa K. Denzin are inventors on patent/patent application 63/183,357 held by Rutgers University that covers the use of Zbtb20 expressing T cells as cellular immunotherapy for inflammatory bowel disease (IBD)

primary activation. Zbtb20$^{+}$ Tregs were enriched in the intestine and specifically expanded when inflammation was induced by the use of DSS. Conditional deletion of *Zbtb20* in T cells resulted in a loss of intestinal epithelial barrier integrity. Consequently, knock-out mice were acutely sensitive to colitis and often died due to the disease. Adoptive transfer of Zbtb20$^{+}$ Tregs protected the Zbtb20 conditional KO mice from severe colitis and death, whereas non-Zbtb20 Tregs did not. Zbtb20 was detected in CD24$^{hi}$, double positive and CD62L$^{lo}$ CD4 single positive thymocytes, suggesting that expression of the transcription factor and the phenotype of these cells were induced during thymic development. However, Zbtb20 expression was not induced in "conventional" Tregs by activation in vitro or in vivo. Thus, Zbtb20 expression identified and controlled the function of a distinct subset of Tregs that are involved in intestinal homeostasis.

## One Sentence Summary

*Zbtb20* expression identifies and is important for the function of a subset of Tregs involved in intestinal integrity.

## Introduction

The BTB-ZF (broad-complex, tramtrack, and bric-à-brac - zinc finger) genes are a family of 49 transcription factors defined by the presence of an N-terminal BTB domain that is involved in protein-protein interactions and C-terminal, DNA binding Krüppel-type zinc fingers (1, 2). BTB-ZF transcription factors control the lineage specification and/or development of key effector functions of lymphocytes (1, 3). The BTB-ZF transcription factor Zbtb1 (*Zbtb1)*, for example, is important for the commitment of developing leukocytes into the lymphoid compartment, and, later in development, another BTB-ZF transcription factor, LRF (Z*btb7a*) is involved in T cell versus B cell lineage commitment (4–6). Other members include ThPOK (*Zbtb7b*) and MAZR (*Zbtb19*) which define the CD4$^{+}$ versus CD8$^{+}$ T cell lineages, respectively (7). PLZF (*Zbtb16*) is crucial for the development of the innate-like effector functions and phenotype of natural killer T cells (NKT) and *Zbtb32* (ROG) is necessary for NK cell proliferation in response to viral infections (3, 8, 9).

BTB-ZF transcription factors are, therefore, important for the development or function of several types of leukocytes (1). Furthermore, the expression of these genes often is restricted to specific subpopulations. Hence, we hypothesized that the discrete expression of BTB-ZF transcription factors in lymphocyte subpopulations might identify new T cell effector populations. Analysis of gene expression reporter mouse models led to the identification of Zbtb20 (*Zbtb20*) as a candidate. Zbtb20 expression identified a distinct subset of FoxP3$^{+}$ regulatory T cells (Tregs).

The specialized immunosuppressive function of Tregs balances and prevents unwanted or excessive immune responses. In doing so, Tregs play an important role in the protection and maintenance of tissues (10). For example, the interplay between the host immune system and the complex network of microbes inhabiting the intestine relies on the activities of Tregs (11). Phenotypic diversity among regulatory T cells (Tregs) suggests the existence of functionally distinct subsets. For example, Foxp3$^{+}$ Tregs that express the IL-33 receptor,

ST2, and the transcription factors, GATA3 and Helios, produce high levels of amphiregulin (Areg), which mediates tissue repair (12). Another subset of Foxp3$^+$ Tregs, defined by expression of RORγt, ICOS, and CTLA-4 has enhanced suppressive capacity during T-cell-mediated intestinal inflammation (13, 14). T-bet expressing Tregs, on the other hand, suppress the responses of Th1 and CD8$^+$ T cells (15). Thus, the tissue-specific milieu and the expression of different transcription factors contribute to the functional diversity of Tregs.

Zbtb20-expressing Tregs had an activated phenotype (CD62L$^{lo}$, CD44$^{hi}$), constitutively expressed *IL10* mRNA, and rapidly secreted the cytokine after primary stimulation. IL-10 is of particular importance for modulating intestinal homeostasis (16–18). Consistent with this, Zbtb20-expressing T cells protected mice from experimental colitis. Zbtb20$^+$ T cells impacted homeostatic maintenance of intestinal integrity as young mice with targeted deletion of *Zbtb20* in T cells had detectable changes in mucosal architecture, inflammation, and an increase in the unrestricted pathways of luminal contents, indicating epithelial cell damage. Although Zbtb20-expressing Tregs were enriched in the intestine, cells with a similar phenotype and ability to produce IL-10 were also found in the thymus and spleen, suggesting that Zbtb20$^+$ Tregs are a committed, rather than an induced, effector population. Collectively, our data show that the transcription factor Zbtb20 identified and controlled a functionally potent subset of regulatory T cells that is important for intestinal homeostasis.

## Results

### Zbtb20 was expressed in discrete T cell subsets

To identify subpopulations of T cells that discretely expressed a BTB-ZF transcription factor, we generated or obtained several bacterial artificial chromosomes (BACs) in which the BTB-ZF gene of interest was replaced by enhanced green fluorescent protein (eGFP). These BACs were then used to generate transgenic mice which were screened for eGFP expression by FACS. Mice carrying a modified ~210kb BAC that was obtained from the Gene Expression Nervous System Atlas (GENSAT) (19) were used to study the expression of Zbtb20. This BAC had an eGFP gene with its own start codon and polyadenylation signal inserted immediately 5' of the *Zbtb20* ATG start site. This design prevented the expression of the BAC-encoded *Zbtb20* gene but retained the regulatory elements and promoter region for *Zbtb20*. qPCR, RNA-Seq, and Western blots of sorted GFP$^+$ and GFP$^-$ T cells showed that eGFP closely mimicked the expression of Zbtb20 (Fig. S1A, B, C, D, E). Also, consistent with published reports of Zbtb20 expression (20), GFP was found in most B1 B cells and some B2 B cells in the peritoneal cavity (Fig. S1F) and Fas$^+$, germinal center B cells in the spleen (Fig. S1G). Combined, these data supported the accuracy of the BAC reporter system.

As detected by GFP expression, ~3% of CD3$^+$ spleen T cells expressed Zbtb20 (ZEG20$^+$ T cells) (Fig. 1A); these cells were CD4$^+$ and ~20% CD25$^+$ (Fig. 1B). ZEG20 mice were crossed to a FoxP3-RFP reporter (21) mouse (ZEG20;FoxP3-RFP) which allowed for detection of both Zbtb20 and FoxP3 expression by FACS. Based on RFP expression, nearly all ZEG20$^+$ CD25$^+$ CD4$^+$ T cells expressed FoxP3. Additionally, more than 30% of ZEG20$^+$ CD25$^-$ CD4$^+$ T cells also expressed FoxP3 as compared to 8% of the non-ZEG20 CD25$^-$

$CD4^+$ T cells (Fig. 1C, D). Similar results were obtained by direct staining for FoxP3 protein in sorted $ZEG20^+$ $CD25^+$ and $ZEG20^+$ $CD25^-$ T cells (Fig. S1H). In total, approximately 50% of $ZEG20^+$ T cells express FoxP3 in healthy mice. Among T cell subsets, Zbtb20 expression was present in spleen $CD4^+$ T cells, $CD4^+CD25^+$ T cells, $CD4^+CD25^-$ T cells, but not in total $CD8^+$ T cells (Fig. 1E). Therefore, using a reporter mouse that identifies Zbtb20 expression in T cells, we found that a small percentage of $CD4^+$ spleen T cells expressed the transcription factor and that nearly half of these cells also expressed FoxP3.

## Zbtb20 was expressed in phenotypically distinct subsets of $CD4^+$ T cells and Tregs

Next, we compared the phenotype and expression of genes in $Zbtb20^+$ Tregs to $Zbtb20^-$ Tregs. Nearly all of the $ZEG20^+$ $Foxp3^+$ Tregs had no expression or reduced levels of CD62L (Fig. 2A). This might have suggested that Zbtb20 was induced simply by activation of Tregs, but, overall, more than half of the $CD62L^{lo}$ Tregs did not express the transcription factor (Fig. 2A). $ZEG20^+CD4^+FoxP3^-$ T cells also had low CD62L expression (Fig. S2A). Gene expression in $ZEG20^+$ Tregs, non-ZEG20 $CD62L^{lo}$ Tregs, and non-ZEG20 $CD62L^{hi}$ Tregs that were sorted from ZEG20;FoxP3-RFP double reporter mice was assessed by RNA-Seq. We focused on the fold change of RNA expression in the phenotypically similar $ZEG20^+$ and non-ZEG20 $CD62L^{lo}$ populations as compared to the larger non-ZEG20 $CD62L^{hi}$ population. This analysis showed that $ZEG20^+$ Tregs expressed 109 genes at higher levels and 85 genes at lower levels as compared to non-ZEG20 $CD62L^{Lo}$ Tregs (Fig. S2B). Several genes, known to be associated with Treg function (22), including *Tigit*, *Tnfrsf18* (GITR), *Klrg1*, *Icos*, *Pdcd1* (PD-1), *Lag3*, *Nrp1* had higher expression in $ZEG20^+$ $FoxP3^+$ Tregs (Fig. 2B). $ZEG20^+$ Tregs also had slightly higher FoxP3 expression (Fig. 2B), which was confirmed by FACS (Fig. S2C). $ZEG20^+$ Tregs had high levels of *Il10* mRNA (Fig. 2B). FACS analysis showed that $ZEG20^+$ $FoxP3^+$ Tregs had the highest expression of CD44, TIGIT, GITR, ICOS as compared to non-ZEG20 $CD62L^{lo}$ or $CD62L^{hi}$ Tregs (Fig. 2C). Similarly, $ZEG20^+$ $FoxP3^-$ $CD4^+$ T cells also had the highest expression of these markers when compared to non-ZEG20 $CD62L^{lo}$ and $CD62L^{hi}$ $CD4^+$ T cells (Fig. S2D). Lastly, FACS analysis with antibodies against common TCR variable regions showed a similar distribution of expression between $ZEG20^+$ and non-ZEG20 Tregs indicating that the Zbtb20-expressing T cells were clonally diverse (Fig. S2E). Phenotypic and genetic analysis, therefore, showed that Tregs that expressed Zbtb20 were distinct from their non-Zbtb20 counterparts.

## Zbtb20-expressing T cells constitutively express *Il10*

The expression of IL-10 is tightly regulated through chromatin structure, histone modification, DNA methylation, and active transcription factors (23). IL-10 is considered to be an effector cytokine that is produced as a result of activation and differentiation of T cells, including Tregs (23). It was unexpected, therefore, that RNA-Seq analysis showed that spleen $ZEG20^+$ Tregs had high levels of *Il10* mRNA directly *ex vivo* (Fig. 2B). To further test *IL10* mRNA levels, we sorted $ZEG20^+$ Tregs and $ZEG20^+$ $CD4^+$ T cells, $CD62L^{lo}$ and $CD62L^{hi}$ non-ZEG20 Tregs, and $CD4^+$ T cells from the spleens of ZEG20;FoxP3-RFP mice. RNA from the sorted cells was isolated, reverse transcribed and the resultant cDNA was used to perform TaqMan based qPCR. $ZEG20^+$ Tregs and $ZEG20^+$ $CD4^+$ T cells had a 100-fold and 30-fold higher *Il10* expression, respectively, as compared to their non-ZEG20

counterparts (Fig. 3A). *Il10* mRNA was also highly expressed in antigen inexperienced thymic ZEG20$^+$ cells (Fig. 3A). Next, the levels of IL-10 secreted by PMA/ionomycin (PMA/ion) activated, FACS sorted ZEG20$^+$ Tregs, non-ZEG20 CD62L$^{lo}$ Tregs, non-ZEG20 CD62L$^{hi}$ Tregs, ZEG20$^+$ CD4$^+$ T cells, and non-ZEG20 CD4$^+$ T cells was determined. ZEG20$^+$ Tregs and ZEG20$^+$ CD4$^+$ T cells produced 3- and 5-fold higher amounts of IL-10 compared to their non-ZEG20 counterparts (Fig. 3B). IL-10 was produced only by the Zbtb20-expressing Tregs following 3 hours of activation (Fig. 3C). Similarly, the secretion of IL-10 was evident for ZEG20$^+$ thymocytes (Fig. 3C). The transcription factor Helios is a marker of thymic derived Tregs that produce high levels of IL-10 (24–27). Therefore, we checked the expression of Helios in ZEG20$^+$ T cells. Approximately 30% of ZEG20$^+$ T cells in the thymus (Fig. 3D) and the spleen (Fig. S3A, B) expressed Helios, however, both Helios$^+$ and Helios$^-$ ZEG20$^+$ T cells were able to secrete IL-10 (Fig. 3D and S3B).

Mice with an IRES-GFP knocked into the 3’ untranslated region of the *IL10* gene were analyzed by FACS. Results showed that a small percentage (~3%) of CD3$^+$ T cells in the spleen expressed GFP, suggesting that the *IL10* locus was in an open configuration in these cells (Fig. S3C). We sorted IL-10-GFP$^+$ Tregs, IL-10-GFP$^-$ Tregs, IL-10-GFP$^+$ CD4$^+$ T cells, and IL-10-GFP$^-$ CD4$^+$ T cells and stained them for Zbtb20 protein expression. Both the Tregs and CD4$^+$ T cells that were IL-10-GFP$^+$ expressed the Zbtb20 (Fig. 3E). Furthermore, the IL-10-GFP$^+$ Tregs had a phenotype similar to ZEG20$^+$ Tregs, with higher expression of CD44, GITR, and TIGIT as compared to non-GFP Tregs (Fig. S3D).

Finally, we used chromatin immunoprecipitation (ChIP) assays to determine if Zbtb20 bound the *IL10* promoter. We identified a human Treg-like T cell line, MT-2, that expresses FoxP3 and IL-10 (28–30). FACS and Western blot analysis showed that MT-2 cells also expressed Zbtb20 (Fig. 3F and S3E). Proteins crosslinked to the chromatin were precipitated with a monoclonal antibody specific for Zbtb20. qPCR was performed using primers amplifying 11 regions 5’ of the IL-10 mRNA transcription start sites, previously identified as accessible to transcription factor binding. Three regions, located at positions −1,810, −6,004, and −12,113 were enriched as compared to an IP with an irrelevant antibody (Fig. 3G). The expression of IL-10 protein by Zbtb20-expressing thymocytes, Tregs, and T cells upon primary activation, the constitutive expression of IL-10 mRNA, and the indication that the IL-10 locus is open in the IL-10-GFP mice suggested that Zbtb20-expressing T cells were “pre-committed” to produce IL-10 without the need for activation induced differentiation. ChIP assays were consistent with the possibility that Zbtb20 might directly control IL-10 production in these cells.

## Enrichment of Zbtb20-expressing Tregs in the gastrointestinal tract

Regulatory T cells (Tregs) use various mechanisms to balance the immune response including the secretion of Interleukin-10 (IL-10), which is of particular importance for modulating intestinal homeostasis (16–18). Since Zbtb20-expressing T cells produced IL-10, we considered the possibility that they accumulate in the intestine. Up to 40% of the small intestine and colon intraepithelial (sIEL and cIEL) Tregs were ZEG20$^+$, as compared to ~15% ZEG20$^+$ Tregs in the spleen from the same mice (Fig. 4A, B, D). The lamina propria lymphocytes (LPL), particularly the colon LPL (cLPL), had more than 50% of

Tregs expressing Zbtb20 (Fig. 4C and D). ZEG20$^{+}$ Tregs were not enriched in the Peyer's Patches (PP) (Fig. 4A and D). Similar to ZEG20$^{+}$ T cells in the spleen and thymus, intestinal ZEG20$^{+}$ T cells also produced substantial amounts of IL-10 (Fig. 4E). These data suggested that Zbtb20-expressing Tregs might have a function in the intestine.

To determine if the Zbtb20$^{+}$ T cells were involved in protecting the intestine from inflammation, we induced colitis in ZEG20 mice by the use of 3% dextran sodium sulfate (DSS) in the drinking water for 5 days followed by a 3-day recovery period (31). On day 8, the cIEL and cLPL were isolated and assessed by FACS. The induction of colitis led to a 3-fold increase in both the frequency and absolute numbers of intraepithelial ZEG20$^{+}$ T cells (Fig. 4F) and a ~20% increase in the percentage and a 2.5-fold increase in the absolute number of ZEG20$^{+}$ T cells in LP (Fig. 4G). The increase in the number of intestinal ZEG20$^{+}$ T cells suggested that ZEG20$^{+}$ T cells, and possibly their IL-10 production, were active participants in the regulation of colitis.

## Deletion of *Zbtb20* in T cells resulted in epithelial layer damage in the intestine

To understand the function of Zbtb20 in T cells, we generated *Zbtb20* conditional knock out (*Zbtb20*-cKO) mice using conventional methods of homologous recombination in embryonic stem (ES) cells derived from C57BL/6 mice. Using a CD4-Cre transgene (32) we deleted *Zbtb20* specifically in T cells during thymocyte development. A FoxP3-GFP reporter gene can label Tregs that develop in mice that have the FoxP3 gene deleted. These so-called "FoxP3 want to be" or, for short "wannabe Tregs are a valuable tool for understanding the features of Tregs that are controlled by FoxP3 (33). We employed a similar strategy by breeding the ZEG20 reporter to CD4-Cre;*Zbtb20*$^{fl/fl}$ mice to produce ZEG20;CD4-Cre;Zbtb20$^{fl/fl}$ (*Zbtb20*-cKO/GFP) mice. We anticipated that even though the gene had been deleted in T cells in these mice, the regulatory elements and promoter region for *Zbtb20* contained in BAC would allow the expression of GFP. Analysis of these "Zbtb20 want to be" T cells (Zbtb20$^{wannabe}$ Tregs and Zbtb20$^{wannabe}$ T cells) collected from *Zbtb20*-cKO/GFP mice provided an ideal means to specifically study the function of the T cells that were potentially altered by the loss of Zbtb20 expression. Importantly, the BAC transgene was constructed such that the *Zbtb20* gene was inactive (19). To confirm that the *Zbtb20* gene was deleted and that protein was not made, we sorted GFP$^{+}$ and GFP$^{-}$ Tregs and CD4$^{+}$ T cells from *Zbtb20*-cKO/GFP and Zbtb20$^{fl/fl}$/GFP (WT/GFP) littermates. PCR of cDNA from these cells showed that the exon flanked by loxP sites was deleted in *Zbtb20*-cKO/GFP mice (Fig. S4A) and FACS analysis showed that Zbtb20$^{wannabe}$ T cells did not express the Zbtb20 protein (Fig. S4B). Combined, these data show that conditional deletion of the gene was efficient.

There was no difference in the total lymphocyte numbers in thymuses and spleens of the *Zbtb20*-cKO/GFP mice when compared to sex-matched WT/GFP mice (Fig. S4C). The frequency of Zbtb20$^{wannabe}$ T cells in the thymus of *Zbtb20*-cKO/GFP mice was, however, decreased by half (Fig. S4D). The number of Zbtb20$^{wannabe}$ T cells was not decreased in the spleen, but fewer of the cells had the activated CD62L$^{lo}$ phenotype (Fig. 5A). There was, however, no change in expression of CD44, GITR, TIGIT, or ICOS (Fig. S4E, F). Sorted Zbtb20$^{wannabes}$ Tregs and Zbtb20 $^{wannabes}$ CD4$^{+}$ T cells from *Zbtb20*-cKO/GFP mice

and ZEG20$^+$ Tregs and ZEG20$^+$ CD4 T cells from WT/GFP mice were next activated *in vitro* with PMA and ionomycin to assess the level of IL-10 production. Consistent with a potential role for Zbtb20 in regulating the production of IL-10, the Zbtb20$^{wannabe}$ Tregs and Zbtb20$^{wannabe}$ T cells secreted ~40% less IL-10 compared to the WT controls (Fig. 5B). There was also a 50% decrease of the Tregs capable to produce IL-10 in *Zbtb20*-cKO mice (Fig. 5C). Thus, Zbtb20 is involved in the development and function of these two T cell populations.

FACS analysis of the colons showed that the frequency of Zbtb20$^{wannabe}$ T cells among IEL and LPL in WT and cKO mice was similar (Fig. S4G) indicating that the deletion of *Zbtb20* did not alter the accumulation of the ZEG20$^+$ T cells. Blinded histological assessment of colons collected from 8-week-old animals showed statistically significant changes in the mucosal architecture in *Zbtb20*-cKO mice with 4.5 fold-higher histological scores in these mice (Fig. 5D). The changes observed in cKO mice included lymphocytic nodules, mild crypt hyperplasia, and mild mucosal edema (Fig. 5D). Several of the *Zbtb20*-cKO mice had increased inflammation, but, overall, these data did not reach significance and the length of the colon was not measurably altered in the cKO mice (Fig. S4H). Next, we tested the integrity of the epithelial barrier by gavage of fasting 14-week-old *Zbtb20*-cKO and WT mice with a mixture of size-selective probes including creatinine, 4 kDa FITC dextran (FD4), and 70 kDa Rhodamine B dextran (RD70). Mice sera collected 5 hours later had elevated levels of all three probes in *Zbtb20*-cKO animals as compared to matched WT controls (Fig. 5E). There was no change in the creatinine/RD70 or FD4/RD70 ratios (Fig. 5G). Combined, these data demonstrated an increase of the unrestricted pathway, which allows particles of any size, including large proteins, viruses, and bacteria to breach the epithelial barrier (34). The flux of luminal contents of this size is a result of the epithelial layer damage (35). Thus, these data were consistent with the damage that was observed in the histology of the intestines in *Zbtb20*-cKO mice. Zbtb20 transcription factor was expressed in both ZEG20$^+$ FoxP3$^+$ and ZEG20$^+$ FoxP3$^-$ T cells thus we used FoxP3-Cre mice to specifically delete the gene only in Tregs (FoxP3-Cre;cKO mice). Results of the gavage experiments, as done above, showed that the mice with Treg specific deletion of *Zbtb20* also experienced epithelial damage that allowed the contents of the intestinal lumen to leave via the unrestricted pathway (Fig. 5F, H). The increase of the three probes was not as high in the mice with *Zbtb20* deletion in Tregs as compared to all T cells which suggested that ZEG20$^+$ Foxp3$^-$ T cells were also involved in the regulation of intestinal homeostasis (Fig. 5F).

## Colitis was exacerbated in *Zbtb20* conditional knock out mice

To further assess the requirement for Zbtb20-expressing T cells in protecting the intestine, we challenged *Zbtb20*-cKO mice with 3% DSS in their drinking water for 5 days followed by a 4-day recovery period. The cKO mice presented with more severe symptoms of colitis including greater loss of body weight (Fig. 6A). Occult blood was also detected in the stool of *Zbtb20*-cKO mice two days earlier than in WT which was consistent with the more severe intestinal inflammation observed in the absence of *Zbtb20* expression in T cells (Fig. S5A, 6D). Additionally, approximately 60% of the cKO mice died post-induction of colitis, whereas all of the wild-type mice recovered from the experimental procedure (Fig. 6B).

The colons of DSS-treated *Zbtb20*-cKO mice that survived were significantly shorter than WT mice (Fig. 6C) and exhibited more severe injury and inflammation (Fig. 6D). Histological assessment of the colons showed substantial ulceration in the *Zbtb20*-cKO mice with approximately 50% of the colonic surface being an ulcer as compared to 25% in WT mice, which was mostly focal (Fig. 6D, underlined). Colons of both WT and *Zbtb20*-cKO mice had atypical hyperplasia of the crypts (marked by arrowheads) and with crypt dilatation (marked by black arrow). Lastly, scoring of inflammatory infiltrates (Fig. 6D white arrow and quantified in bar graphs) revealed a high density of transmural lymphocyte infiltration (size of GALT >50%) and severe epithelial exfoliation in the cKO mice, with less florid transmural inflammation (size of GALT 20–50%) and focal exfoliation observed in WT mice throughout the sections shown (Fig. 6D). Mice with the FoxP3-Cre deletion of *Zbtb20* also experienced more severe symptoms from DSS-induced colitis (Fig. 6E) which resulted in the death of about half of the cKO mice and shortened colon length in the surviving FoxP3-Cre;cKO mice (Fig. 6F). The consequences of deletion of *Zbtb20* with FoxP3-Cre overall were less severe than deletion with CD4-Cre (Fig. 6E and F), which again suggested that the Zbtb20-expressing $CD4^+$ T cells also played an active role in suppressing inflammation.

FACS analysis of cells collected from colons of mice with DSS-induced colitis showed that the numbers of $ZEG20^+$ T cells and $Zbtb20^{wannabe}$ T cells similarly increased in both the epithelium and LP (Fig. S5B), while Non-Treg, non-Zbtb20-expressing $CD3^+$ T cells increased only in the *Zbtb20*-cKO mice (Fig. S5C). Combined these results indicated that the exacerbated severity of colitis in mice with the deletion of *Zbtb20* in T cells, specifically Tregs, was most likely due to changes in the function of the cells (e.g. decrease in IL-10 production), rather than a change in the frequency, of the $Zbtb20^{wannabe}$ T cells in the intestine.

## Adoptive transfer of Zbtb20-expressing Tregs rescued the cKO mice with colitis

Next, we asked if $Zbtb20^+$ Tregs might be more effective than “conventional” non-Zbtb20 Tregs in protecting or rescuing mice from DSS-induced colitis. We adoptively transferred of $5\times10^5$ total Tregs (both Zbtb20-expressing and not expressing) from WT mice into *Zbtb20*-cKO mice one day before treatment with DSS. This transfer resulted in the progression of the disease and bodyweight change that closely resembled WT mice (Fig. 7A). Transfer of $1\times10^5$ sorted $ZEG20^+$ Tregs also rescued the cKO mice from weight loss and death after colitis induction (Fig. 7B). On the other hand, the transfer of $1\times10^5$ non-Zbtb20 Tregs was not sufficient to rescue the cKO mice (Fig. 7B). Of note, 100% of the *Zbtb20*-cKO mice that received $1\times10^5$ $ZEG20^+$ Tregs survived colitis, whereas 40% of the mice that received the Tregs depleted of the Zbtb20-expressing T cells (non-ZEG20 Tregs) died (Fig. 7B). The transfer of a larger number of non-ZEG20 Tregs ($5\times10^5$) was able to rescue the cKO mice, suggesting that $Zbtb20^+$ Tregs were more effective in suppressing the inflammation (Fig. S6).

IL-10 is essential in controlling intestinal inflammation (16–18). We crossed the ZEG20 mice with IL-10 deficient mice to interrogate the importance of IL-10 specifically produced by $ZEG20^+$ T cells. To test this, $ZEG20^+$ $IL\text{-}10^{-/-}$ Tregs were adoptively transferred into

*Zbtb20*-cKO mice followed by treatment with DSS. The cKO mice that received IL-10 deficient ZEG20$^+$ Tregs had excessive weight loss and 30% succumbed to the disease (Fig. 7C). Colitis was not as severe in these mice though, suggesting that IL-10 production was not the only means by which Zbtb20-expressing Tregs protected the intestine. Therefore, although IL-10 can be produced by many different cell types (36), IL-10 expression specifically in Zbtb20-expressing Tregs played a role in protecting the intestine. Overall, these data showed that Zbtb20-expressing Tregs, partly due to the production of IL-10, were more effective than non-Zbtb20 Tregs at rescuing mice from colitis.

## Induction of Zbtb20 occurred during thymic development

Although intestinal Tregs are phenotypically diverse, they can be broadly divided into thymus-derived or peripherally induced Treg subsets (37, 38). The prominent subtype of Treg in the colon appears to be induced, possibly resulting from activation of conventional CD4$^+$ T cells by antigens derived from commensal bacteria (39). This conclusion is consistent with the finding that the frequency of Tregs in mice devoid of microbiota is markedly reduced (40, 41). To determine if Zbtb20 was peripherally induced, we utilized different T cell activation strategies followed by FACS to assess the expression of Zbtb20. First, total T cells in single-cell suspensions of spleens from ZEG20 mice were activated, *in vitro*, with antibodies against CD3 for four days. Compared to the input, there was no increase of eGFP positive cells among CD4$^+$ T cells and CD8$^+$ T cells, which did not express Zbtb20 to start and remained negative (Fig. S7A, B). To determine if Zbtb20 was induced upon activation of differentiated T cells, we rested the T cells for a total of 6 days and then reactivated with anti-CD3/anti-CD28 beads for four more days. As for the primary activation, the secondary activation did not induce additional Zbtb20 expression in CD4$^+$ T cells. CD8$^+$ T cells remained negative for Zbtb20 expression (Fig. S7B). Addition of exogenous TGFβ and IL-6 during the activation, which induces FoxP3 expression (42), also did not induce Zbtb20 expression (Fig. S7C). Next, allelically marked (CD45.2), FACS sorted eGFP negative CD4$^+$ spleen T cells from ZEG20 mice were adoptively transferred into CD45.1 (B6.SJL) host mice. After two weeks, lymphocytes were isolated from the Peyer's Patches, and the transferred CD45.2$^+$ T cells were analyzed by FACS. GFP expression was not detected in these cells (Fig. S8A). Lastly, we transferred FACS sorted GFP negative CD4SP thymocytes into B6.SJL host mice. We used thymocytes with the expectation that more immature cells were less likely to already have committed to a specific lineage. Mice were treated with DSS to induce colitis and activate T cells. Ten days post-induction, spleen and intestinal T cells were analyzed by FACS (Fig. S8B). Induction of GFP in the donor cells was not detected.

Since Zbtb20 induction was not observed following T cell activation in the periphery, we next asked if the transcription factor was induced during thymic development. FACS analysis showed that Zbtb20 was expressed in CD3$^{hi}$CD4$^+$CD8$^-$ single-positive cells (CD4SP), but not in CD8SP thymocytes (Fig. 8A). Zbtb20 was also expressed in very immature CD3$^{lo}$CD4$^+$CD8$^+$CD24$^+$DP (double positive) thymocytes (Fig. 8C, S9A). Peripheral Tregs that migrate back to the thymus tend to express CD73 (43). Approximately half of the ZEG20$^+$ CD4SP thymocytes were negative for CD73 (Fig. 8B), which was comparable to the number previously reported for the total FoxP3$^+$ CD4SP population (43).

This suggested that not all the ZEG20$^+$ CD4SP were mature cells that had trafficked back to the thymus. ~30% of ZEG20$^+$ CD4SP cells expressed CD25 and ~30% of the ZEG20$^+$ CD25$^-$ CD4SP cells expressed FoxP3 (Fig. 8D). ZEG20$^+$ CD4SP thymocytes expressed low levels of CD62L suggesting that this phenotype was induced during development, rather than as a consequence of peripheral activation (Fig. 8C). Despite the CD73 staining, it was still possible that Zbtb20-expressing Tregs in the thymus were mature cells that recirculated from the periphery. To eliminate this possibility, we did fetal thymic organ culture (FTOC) with thymuses taken from ZEG20 mouse fetuses or WT controls. Thymocytes were analyzed after 14 days of culture. Only CD4SP cells from the reporter thymuses expressed GFP, directly showing that Zbtb20 could be induced during T cells development (Fig. S9B). Of note, the low expression of Zbtb20 may have been a consequence of cells not reaching full maturity in FTOC. Combined, these data suggested that Zbtb20-expressing T cells were a thymic-derived subset rather than an activation-induced derivative of peripheral conventional T cells. This was further supported by the fact that both FoxP3$^+$ and FoxP3$^-$ Zbtb20$^+$ T cells expressed Neuropilin-1 (Nrp-1) (Fig. 2B, 8E and F), a marker of thymus-derived Tregs (44–46).

## Discussion

Here, we identified a subset of T cells that expressed the BTB-ZF transcription factor, *Zbtb20*. Half of these T cells expressed FoxP3 and the population constitutively transcribed *IL10* and produced the cytokine upon primary activation. Zbtb20$^+$ Tregs were enriched in the large intestine and specifically expanded during experimental colitis. *Zbtb20* conditional knock out mice had substantially more intestinal inflammation and damage in response to induction of acute colitis. Indeed, the severity of the disease often led to the death of the cKO mice. Adoptive transfer of sorted Zbtb20-expressing Tregs prevented the exacerbated weight loss and mortality in *Zbtb20*-cKO mice, whereas the transfer of non-Zbtb20-expressing Tregs did not. Combined, these data showed that protection from disease was directly attributed to Zbtb20$^+$ Tregs. Therefore, Zbtb20$^+$ Tregs had protective abilities in the intestine that complement the overall function of the Treg population.

Tregs in the intestine are required for maintaining tolerance to dietary antigens, commensal organisms, and pathogens (47). Tregs also play an active role in homeostasis, tissue repair, and epithelial barrier functions. To manage this array of responsibilities, gut-resident Tregs are phenotypically and functionally heterogeneous and develop by diverse means (47, 48). Many intestinal Tregs acquire their functionality *in situ* following activation by microbial antigens (49) (50). Zbtb20$^+$ Tregs, however, were a distinct, thymic-derived population. This conclusion was drawn both from data showing that Zbtb20 was not induced by activation of peripheral Tregs and that Zbtb20 was first expressed at a very early stage of thymic development (CD24$^{hi}$CD3$^{lo}$DP). Zbtb20$^+$ Tregs also appeared to be distinct in that they had the capacity to produce IL-10 upon primary activation as compared to the other intestinal Tregs that secrete the cytokine as a result of differentiation upon peripheral activation (23, 51).

The regulation of *IL10* transcription is complex, with different chromatin organization in different cell types (23, 52). Our data suggest that in Zbtb20$^+$ T cells, IL-10 transcription

might be directly controlled by Zbtb20 since the transcription factor occupies at least three sites in the promoter region. *IL10* mRNA and protein were evident in Zbtb20-expressing thymocytes, which implied that this was a "hard-wired" cell intrinsic function that likely was maintained throughout the life of the cell. Experiments showed that IL-10 deficient Zbtb20$^+$ Tregs were unable to rescue *Zbtb20*-cKO mice from severe colitis. Therefore, despite the abundant number and variety of other cells that can produce IL-10 in the intestine, the IL-10 produced by Zbtb20$^+$ Tregs was important.

While the severe outcomes of induced colitis were dramatic, the more subtle impact that loss of *Zbtb20* in T cells had on the maintenance of the intestinal epithelial barrier (IEB) integrity may ultimately be of greater importance. The IEB has multiple functions including preventing the release of potentially harmful pathogens and antigens, while also directly aiding in the absorption of nutrients and water (53). As such, IEB integrity is associated with a broad range of diseases including inflammatory bowel disease, irritable bowel syndrome, and even Celiac Disease (54–56). A complete loss of *Zbtb20* expression in T cells resulted in a measurable increase of the unrestricted pathway, which is distinct from both the paracellular and transcellular pathways that have charge- and size-selectivity (57) and directly indicated IEB damage in young (8-week old), otherwise healthy mice. Therefore, it is tempting to speculate that reduced activity or frequency of Zbtb20$^+$ Tregs might be associated with cumulative IEB damage over time leading to a predisposition for the diseases like those mentioned above.

Several of the 49 BTB-ZF transcription factors fit the definition of "master regulators"; genes that occupy the top of a regulatory hierarchy and are essential for the development of a lineage or cell type (58). We propose that Zbtb20 should be added to this list since, in T cells, its expression was induced very early in development, it defined a type of T cell that, in the absence of the gene, lose their distinctive functions. It will be interesting to see if like ThPOK, PLZF, and Bcl6 (1), the characteristics of Zbtb20$^+$ T cells can be transferred to other T cells via ectopic expression of the transcription factor. In addition to iNKT cells, PLZF also controls several other innate-like cells that are broadly linked to the Type II immune response, such as ILC2s, basophils, MAIT cells, and others (59–62). In these cells, PLZF generally controls the ability to rapidly produce cytokines upon primary activation. Zbtb20 is also expressed in other cell types (20, 63–65). It will be interesting to learn if, like PLZF, there is a commonality to its function in these cells.

Our screen for new T cell effector populations identified a functionally and phenotypically distinct T cell lineage defined by expression of the BTB-ZF gene, *Zbtb20*. Zbtb20 impacts the function of other cells including some B cells, some myeloid cells, and, possibly indirectly, CD8$^+$ T cells (20, 63–65). Our data suggested that Zbtb20$^+$ Tregs are a player in the complex network of cells that control intestinal homeostasis. However, unlike many other cell types which acquire their specific functions *in situ*, Zbtb20-expressing T cells can be detected outside of the intestine. Therefore, monitoring the frequency or function of these cells may prove to be a biomarker for the risk of IBD development.

## Methods and Materials

### Study Design

The objective of this study was to determine the phenotype and function of a subset of regulatory T cells that express the transcription factor, *Zbtb20*. Genetic reporter mice were used to isolate the Tregs and to determine gene expression and function. Mice with a genetically induced deletion of Zbtb20 were tested for the onset of colitis. Experiments were done three or more times, as indicated in the figure legends. Sample sizes were determined on the basis of power calculations, guided by earlier similar studies from our laboratory. Outliers were not excluded. Male and female were used, with no statically significant differences in results. Observational studies, such as pathology reports were carried out by blinded, the third party not involved in the study.

### Mice

Zbtb20-eGFP reporter mice (ZEG20) were made with an engineered BAC obtained from the Gene Expression Nervous System Atlas (GENSAT) (19) and microinjected into fertilized C57BL/6 eggs by MSKCC's Mouse Genetics Core Facility. The resulting founders were backcrossed to C57BL/6 mice and screened for GFP expression by FACS. Multiple founders showed similar expression and one was selected for further study. The CD4-Cre, Foxp3$^{i\textit{res-mrfp}}$ (FIR), IL-10$^{\textit{ires-GFP}}$ (tiger), RAG1$^{-/-}$, C57Bl/6, B6.CD4-Cre, B6.129P2-Il10$^{tm1Cgn}$/J, B6.129(Cg)-Foxp3t$^{m4(YFP/icre)Ayr}$/J (Foxp3$^{YFP\text{-}cre}$), and B6.SJL mice were purchased from The Jackson Laboratory (Bar Harbor, ME). Zbtb20$^{flox/flox}$ mice were generated by Dr. Lynn Corcoran's laboratory (The Walter and Eliza Hall Institute of Medical Research) using conventional methods of homologous recombination in embryonic stem (ES) cells derived from C57BL/6 mice. The targeting vector contained 5.4kb (5') and 4.2kb (3') of homologous Zbtb20 genomic sequence flanking a 1605bp central protein-coding exon, which was flanked by loxP sites. In these mice, Cre-mediated recombinase deletes exon 14 (Transcript: Zbtb20–204 ENSMUST00000114694.8), resulting in a Zbtb20 protein lacking 535 central residues, including the BTB/POZ domain and the first Zn finger.

Unless otherwise mentioned, experiments were done using 8–12-week-old mice (age- and sex-matched). Both sexes were included to account for possible biological variability. Mice were co-housed at least 4 weeks before each experiment to account for potential differences in the microbiome. Mice were euthanized by carbon dioxide asphyxiation, followed by cervical dislocation. Mice were in the CHINJ animal facility. Animal care and experimental procedures were carried out following the guidelines of the Institutional Animal Care and Use Committee of Rutgers University and the National Institutes of Health Guide for the Care and Use of Laboratory Animals. The loss of 30% of starting weight was specifically approved by the IACUC once shown to be a scientific necessity.

### Cell isolation

Thymuses, spleens, and PPs were dissociated between glass slides, filtered through a 40-μm mesh, and treated with RBC Lysing Buffer (Sigma-Aldrich) to obtain single-cell suspensions. Small intestines and colons were longitudinally opened, rinsed in $Ca^{2+}$- and $Mg^{2+}$-free HBSS (Sigma-Aldrich), and incubated on a shaker (at 250 rpm), in HBSS

with 5% (wt/vol) heat-inactivated FBS (HI FBS) (Gibco) and 2mM EDTA, 1h at 37°C. Cell suspensions were filtered through a 100-μm mesh then applied to nylon wool packed columns to remove debris. LP leukocytes were isolated by two 20 min digestions with 100U/mL and 200U/mL of Collagenase type IV (Worthington) in RPMI (Gibco) with 5% (wt/vol) HI FBS.

## Flow Cytometry and cell sorting

Cells were stained for 30 min at 4 °C in FACS buffer (PBS with 1% HI FBS) after blocking with 2% mouse serum, 0.1% anti-Fcγ Ab, and 0.1mg/mL streptavidin (20 min at 4 °C). Intracellular staining was done with the FoxP3/Transcription Factor Staining Buffer Set (eBioscience). The following antibodies were used: anti-CD4 (RM4–5)(GK1.5), anti-CD62L (MEL-14), anti-Zbtb20 (4A3), anti-CD11b (M1/70), anti-CD80 (16–10A), anti-FAS (Jo2), anti-CD19 (1D3), anti-CD5 (53–7.3) anti-TCR Valpha2 (B20.1), anti-TCR Valpha3.2b and 3.2c (RR3–16), anti-TCR Valpha8 (B24), anti-TCR Vbeta6 (RR4–7), anti-TCR Vbeta7 (TR310), anti-TCR Vbeta8 (F23.1) (BD Bioscience). Anti-CD44 (IM7), anti-CD45.2 (104), anti-CD45.1(A20), anti-CD3 (500.A2), anti-CD24 (16–10A), anti-CD25 (PC61)(PC61.5), anti-CD69 (H1.2F3), anti-CD8 (53–6.7), anti-ICOS (15F9), anti-GITR (DTA-1), anti-FoxP3 (FJK-16s), anti-TIGIT (GIGD7), anti-CD73 (eBioR2/60), anti-IgM (11/41) and anti-Neuropilin-1 (3DS304M) (eBioscience). Anti-Ly-6C (16–10A), anti-F4/80 (16–10A), anti-CX3CR1 (16–10A), anti-CD103 (16–10A) and anti-Helios (16–10A) (BioLegend). Anti-MHC II (212.A1) was generated by the MSKCC Ab Core Facility. Dead cells were excluded by DAPI staining or Bioscience™ Fixable Viability Dye eFluor™ 506, Doublets were excluded by comparing FSC width to height. LSRII (BD Biosciences) or Cytek™ Aurora cytometers were used. Data were analyzed with FlowJo software (TreeStar, Ashland, OR). Cell sorting was done on either Miltenyi autoMACS PROseperator or BD Influx.

## RNA-Seq analysis

Spleen cells from four ZEG20;FoxP3-RFP double reporter mice were sorted using the expression of GFP, RFP, CD62L, and CD4 to obtain highly pure (~99%) populations of Zbtb20$^{+}$ FoxP3$^{+}$ Tregs, Zbtb20$^{-}$ FoxP3$^{+}$ CD62L$^{Lo}$ Tregs, and Zbtb20$^{-}$ FoxP3$^{+}$ CD62L$^{Hi}$ Tregs. Approximately $1 \times 10^{5}$ cells were resuspended in 100μL of TRIzol (Sigma-Aldrich) solution and stored at −80°C until the RNA extraction. RNA was isolated from the cell using the Direct-zol RNA MicroPrep Kit (Zymo Research). RNA quality, SMARTer mRNA Amplification, libraries preparation, and RNA-Seq was done at the Lewis-Sigler Institute for Integrative Genomics, Princeton University. Sequencing was done on an Illumina HiSeq 2500 in Rapid mode as one lane of single-end 75nt reads following the standard protocol. Raw sequencing reads were filtered by Illumina HiSeq Control Software and yielded about 160 million Pass-Filter (PF) reads for further analysis. PF Reads were de-multiplexed using the Barcode Splitter in FASTX-toolkit, and the reads from each library were mapped to the mouse genome. The htseq-count software was used next to obtain gene expression value as the total number of reads mapped to all exons of each gene, and these counts were further normalized to minimize the variation among samples and log2-transformed after raising all zero values to 0.5 to obtain a log2-fold change between each pair of samples. Heat maps were generated using GraphPad Prism (La Jolla, CA) software.

## qPCR and RT-PCR

Cells were FACS sorted to obtain >98% purity of $GFP^+$ and $GFP^-$ cells. RNA purification and cDNA synthesis were carried out with the Qiagen RNeasy kit (gDNA shredder), GoScript™ Reverse Transcription, and random hexamers (Promega). The resultant cDNA was used to perform TaqMan (Life Technologies) based qPCR with TaqMan β2M (Mm00437762_m1), IL-10 (Mm01288386) and Zbtb20 (Mm00457764_m1) probes, and TaqMan Universal PCR Master Mix No AmpErase UNG (Life Technologies). Samples were run on a QuantStudio6 Flex Real-Time PCR System (Life Technologies). Data were normalized to β2M and expressed as a relative target amount using the ΔΔCT method. *Zbtb20* expression in sorted $GFP^+$ and $GFP^-$ cells, collected from ZEG20 and *Zbtb20*-cKO/GFP mice were assessed using Taq2X Master Mix (NB BioLabs) and primers designed in our laboratory (Table 1). The PCR products were run on 1% agarose (Hoefer) gel and imaged using Kodak's Logic 200 Imaging System.

## Western Blots

T cells and B cells from the spleen of ZEG20 mice were sorted to >98% purity of $GFP^+$ and $GFP^-$ cells. 150 $\times 10^3$ T cells and 25 $\times$ $10^3$ B cell were lysed with buffer containing 25 mM Tris•HCl pH 7.6, 150mM NaCl, 1% NP-40, 1% sodium deoxycholate, 0.2% SDS. Equal amounts of protein were separated by 8% SDS-PAGE gels and transferred to polyvinylidene fluoride membrane (Millipore). Membranes were probed with anti-Zbtb20 antibody (clone: 7C8; made by L.M.C. and anti-b-Actin Clone AC-15 (Sigma A5441).

T-cell line MT-2, acquired from the AIDS Research and Reference Reagent Program of the National Institutes of Health (Rockville, MD) and Jurkat T cell line (ATCC TIB-152), were grown in RPMI 1640 (Life Technologies) supplemented with 10% FBS (Gemini Bio-Products), 100u/ml Penicillin/Streptomycin (Life Technologies), 2mM GlutaMAX-1 (Life Technologies), and 10 mM HEPES (Life Technologies).

MT-2 and Jurkat cells were lysed in hypotonic lysis buffer: 0.2% NP-40, 10mM HEPES, 1.5mM MgCl2, 10mM KCl, 5mM EDTA, and protease inhibitor cocktail; nuclei were pelleted then resuspended with lysis buffer: 20mM HEPES, 300mM NaCl, 20mM KCl, 0.05% NP40, protease inhibitor cocktail. Equal amounts of lysates were separated by 8% SDS-PAGE gels and transferred to polyvinylidene fluoride membrane (Millipore) and probed with anti-Zbtb20 (clone: 7C8) and anti-HDAC1 (Cell signaling). After washing, blots were developed with HyGlo chemiluminescent HRP detection reagent (Denville Scientific) and exposed to autoradiography film followed by film development using X-ray film processor (Kodak). The images were captured by scanning the developed film.

## Chromatin immunoprecipitation

ChromaFlash High-Sensitivity ChIP Kit (Epigentek p-2027) was used with anti-ZBTB20 (clone: 4A3) Rat IgG2a antibody (made by L.M.C.) and non-specific isotype control, anti-H2M 2C3M Rat IgG2a antibody. MT-2 cells were cross-linked with 1% formaldehyde (Sigma-Aldrich F8775), for 10 min at room temperature, and quenched with 125mM glycine, sonicated on ice and the fragmented chromatin was immunoprecipitated using 4μg anti-Zbtb20. RT- PCR was performed with PowerUp SYBR Green Master Mix (Thermo

Fisher Scientific). Three independent ChIPs were done. Primers (Table 1) were chosen based on DNAse hypersensitivity and ChIP-seq data presented on the UCSC Genome Browser for the Human, Feb. 2009 (GRCh37/hg/19) Assembly.

## Cytokine Bead Array

$5\times10^4$ (Fig. 5) or $2\times10^5$ (Fig. 3) sorted T cells were stimulated with Phorbol 12-myristate 13-acetate (PMA) (Sigma-Aldrich) (100ng/mL) and ionomycin (Sigma-Aldrich) (500ng/mL). Supernatants were collected after 24 hours. Cytokines were measured with BD Cytometric Bead Array as recommended.

## IL-10 Secretion Assay

The Mouse IL-10 Secretion Assay (Miltenyi Biotec) was used as recommended. $20\times10^6$ cells were stimulated with PMA (100ng/mL) and ionomycin (500ng/mL) at $37^0$C for 3h, washed, and incubated with the anti-IL-10 capture antibody for an additional 45 min. Cells were stained with the IL-10 detection antibodies, anti-CD25, anti-CD4, anti-CD3, and anti-CD62L and analyzed by FACS.

## Histology

The collection and preparation of the intestine for the histological analysis was done as described in Bialkowska et al., 2016 (66). The colons of 8-week old *Zbtb20*-cKO and WT mice were harvested and gently rinsed with modified Bouin's fixative (a mixture of 50% ethanol and 5% acetic acid in water) using a 10-mL syringe filled and a gavage needle. Swiss rolls were fixed in 10% buffered formalin overnight at room temperature, next rinsed, and stored in 70% ethanol at 4ºC. The embedding in paraffin, sectioning (5μm), and hematoxylin and eosin staining of the colons was done by Nationwide Histology LLC. The pathologists at Nationwide Histology LLC performed also blinded histological evaluation and scoring of the severity of the colitis as described in Koelink PJ. et al., 2018 (67), Kim JJ. et al., 2012 (68) and Erben U. et al. (69). Disease severity was scored from 0 to 5, where 0 is a healthy colon and 5 severe colitis (histological and inflammation scores). The histological evaluation was further confirmed and photographed by A.B.R. at the Rutgers Child Health Institute of NJ.

## Intestinal permeability

The intestinal permeability assay was performed as described before by Edelblum KL et al., 2017 (35). 14-week old *Zbtb20*-cKO and WT mice were fasted for 2 hours and then gavaged with a mixture of 100 mg/mL creatinine (Sigma C4255), 80 mg/mL FITC-dextran 4kDa (FD4) (Sigma 46944), and 20 mg/mL Rhodamine B-dextran 70 kDa (Sigma R9379). After 5h the 250–300μL of blood was collected by the retroorbital bleed. Samples were spun down at 1000 RPMs and ~100μL of serum was collected for the analysis. Fluorescence intensity for FD4 and RD70 was determined by using a plate reader at 495 nm excitation/525 nm emission and 555 nm excitation/585 nm emission, respectively. The concentration of creatinine was measured using the Sciteck SVT creatinine kit (Sciteck 139–30) according to the manufacturer's protocol.

### Dextran sodium sulfate treatment

The DSS-induced colitis model was done as described before (31). Briefly, mice received 3% colitis grade DSS (MP Biomedicals) in drinking water for 5 days and regular water for an additional 2–6 days. The body weight of the mice was assessed daily and presented as a percent of the initial weight. The presence of the occult blood in the stool was detected with the Hemoccult II test (Sensa).

### Treg adoptive transfer and colitis rescue experiments

Total Tregs from spleens were isolated using the $CD4^+$ $CD25^+$ Regulatory T Cell Isolation Kit (Miltenyi Biotec) and autoMACS PROseperator. The cells were washed 3 times with sterile PBS and $5\times10^5$ were resuspended in 200μL of sterile saline. Tregs were i.p. injected with a 1 mL sterile sub-Q syringe 26 G, one day before induction of the colitis with 3% DSS. Treg subpopulations were sorted from the spleens of ZEG20;FoxP3-RFP double reporter mice or ZEG20/IL-$10^{-/-}$ mice. $1\times10^5$ or $5\times10^5$ of the sorted cells were resuspended in 200μL of sterile saline and i.p. injected into Zbtb20 cKO mice one day before induction of colitis.

### Fetal thymic organ culture (FTOC)

Timed breeding of ZEG20 reporter males with B6 WT females was set up. Thymic lobes of E16 embryos were collected, placed in transwell plates (Costar; 0.4 μ m pore size) and cultured in DMEM supplemented with 10% HI FBS for 14 days (according to Current Protocols in Immunology). The cells were FACS analyzed for expression of surface markers (CD45.2, CD3, CD4, CD8 CD25, Thy1) and GFP. The genotype of each embryo was determined by PCR.

### *In vitro* induction of Zbtb20

$2\times10^6$ of total splenocytes from ZEG20 mice were activated by adding 2.5 μg/mL anti-CD3 (purified 2C11) in RPMI containing 5% HI FBS. After 96h cells were stained with anti-CD3, anti-CD8, anti-CD4, anti-CD44, anti-CD62L, anti-MHC II and analyzed by FACS for the presence of $GFP^+$ T cells. The remaining cells were reactivated 6 days later with anti-CD3/CD28 microbeads at 1:1 bead:cell ratio (mouse T Cell Activation/Expansion Kit, Militenyi) in RPMI containing 5% HI FBS and 50 U/ml IL-2. After 96h cells were stained and FACS analyzed as described above.

$2\times10^6$ of sorted $GFP^-$ $CD4^+$ T cells from ZEG20 mice were activated for 72h with 5 μg/ml plate-bound anti-CD3 (2C11) and soluble anti-CD28. The cells were cultured in RPMI containing 5% HI FBS and 50 U/ml IL-2, supplemented with 20 ng/mL IL-6, 5 ng/mL TGF-β, or both. After 72h cells were FACS analyzed as described above.

### *In vivo* induction of Zbtb20

$GFP^-$ $CD4^+$ $CD45.2^+$ T cells from spleens of ZEG20;FoxP3-RFP double reporter mice were sorted and $3\times10^6$ of the cells were i.p. injected into B6.SJL mice ($CD45.1^+$, non-GFP recipient). After 2 weeks, the recipient mice were sacrificed and lymphocytes from intestines

were isolated and stained with anti-CD45.2, anti-CD45.1, anti-CD3, anti-CD4, anti-CD8, anti-CD62L, anti-MHC II and analyzed by FACS for the presence of $GFP^+$ T cells.

$GFP^-$ CD4SP $CD45.2^+$ thymocytes from ZEG20;FoxP3-RFP double reporter mice were sorted and $2\times10^6$ of the cells were i.p. injected into B6.SJL/B6 mice ($CD45.1^+/CD45.2^+$, non-GFP recipient). The next day the recipient mice received 3% DSS for 6 days following 3 days of recovery. Cells from the spleen, PPs, small intestine, and colon were collected on day 10 post-injection and FACS analyzed as described above.

### Statistical analysis

Data from at least three samples in two or more independent experiments were collected as detailed in the figure legends. Statistical analysis was performed using GraphPad Prism (La Jolla, CA) software. Data were expressed as the mean; error bars represent ± SEM. Unpaired t-tests were used when two groups were compared. One-way ANOVA with Tukey correction was used for the comparison of three or more groups. Two-way ANOVA with Tukey correction was used for changes in body weight. P values $<0.05$ were considered significant. * $P<0.05$, ** $P<0.01$, *** $P<0.001$.

## Supplementary Material

Refer to Web version on PubMed Central for supplementary material.

## Acknowledgments

This study was supported by NIH NIAID R01 AI122757, the Robert Wood Johnson Foundation (grant #67038) to the Child Health Institute of New Jersey, The Harold L. Paz, M.D. Endowed Professor of Developmental Biology, New Jersey Health Foundation's Excellence in Research Award (to D.B.S.) and the Century for the Cure Foundation. Services in support of the research were generated by the Rutgers Cancer Institute of New Jersey Flow Cytometry & Cell Sorting Shared Resource, the Genome Editing Shared Resource, and the Biomedical Informatics Shared Resource (P30CA072720–5921, −5922 and −5917, respectively), and the Comparative Medicine Resources and the Immune Monitoring Shared Resource. We thank Danielle Millick, Patrick Darcy, Joshua Vieth, and Austin Graves (CHINJ) for critical analysis of the data and/or help with experimental procedures; Arthur Roberts for cell sorting and Dr. Ying Chen for RNA-Seq data processing and analysis (CINJ); Dr. Wei Wang for RNA-Seq analysis (Princeton University) and Dr. Deepta Bhattacharya (The University of Arizona) for kindly providing the $Zbtb20^{flox/flox}$ breeding pairs.

## Data and material availability

RNA-Seq data generated in this study are deposited in ArrayExpress under accession number E-MTAB-11442. All data needed to evaluate the conclusions in the paper are present in the paper or the Supplementary Materials.

## References and notes

1. Beaulieu AM, Sant'Angelo DB, The BTB-ZF family of transcription factors: key regulators of lineage commitment and effector function development in the immune system. J Immunol 187, 2841–2847 (2011). [PubMed: 21900183]
2. Chevrier S, Corcoran LM, BTB-ZF transcription factors, a growing family of regulators of early and late B-cell development. Immunol Cell Biol 92, 481–488 (2014). [PubMed: 24638067]
3. Kovalovsky D et al. , The BTB-zinc finger transcriptional regulator PLZF controls the development of invariant natural killer T cell effector functions. Nat Immunol 9, 1055–1064 (2008). [PubMed: 18660811]

4. Maeda T et al. , Regulation of B versus T lymphoid lineage fate decision by the proto-oncogene LRF. Science 316, 860–866 (2007). [PubMed: 17495164]
5. Siggs OM, Li X, Xia Y, Beutler B, ZBTB1 is a determinant of lymphoid development. J Exp Med 209, 19–27 (2012). [PubMed: 22201126]
6. Zhang X, Lu Y, Cao X, Zhen T, Kovalovsky D, Zbtb1 prevents default myeloid differentiation of lymphoid-primed multipotent progenitors. Oncotarget 7, 58768–58778 (2016). [PubMed: 27542215]
7. He X et al. , The zinc finger transcription factor Th-POK regulates CD4 versus CD8 T-cell lineage commitment. Nature 433, 826–833 (2005). [PubMed: 15729333]
8. Savage AK et al. , The transcription factor PLZF directs the effector program of the NKT cell lineage. Immunity 29, 391–403 (2008). [PubMed: 18703361]
9. Beaulieu AM, Zawislak CL, Nakayama T, Sun JC, The transcription factor Zbtb32 controls the proliferative burst of virus-specific natural killer cells responding to infection. Nat Immunol 15, 546–553 (2014). [PubMed: 24747678]
10. Campbell C, Rudensky A, Roles of Regulatory T Cells in Tissue Pathophysiology and Metabolism. Cell Metab 31, 18–25 (2020). [PubMed: 31607562]
11. Jacobse J, Li J, Rings E, Samsom JN, Goettel JA, Intestinal Regulatory T Cells as Specialized Tissue-Restricted Immune Cells in Intestinal Immune Homeostasis and Disease. Front Immunol 12, 716499 (2021). [PubMed: 34421921]
12. Sharma A, Rudra D, Emerging Functions of Regulatory T Cells in Tissue Homeostasis. Front Immunol 9, 883 (2018). [PubMed: 29887862]
13. Sefik E et al. , MUCOSAL IMMUNOLOGY. Individual intestinal symbionts induce a distinct population of RORgamma(+) regulatory T cells. Science 349, 993–997 (2015). [PubMed: 26272906]
14. Ohnmacht C et al. , MUCOSAL IMMUNOLOGY. The microbiota regulates type 2 immunity through RORgammat(+) T cells. Science 349, 989–993 (2015). [PubMed: 26160380]
15. Levine AG et al. , Stability and function of regulatory T cells expressing the transcription factor T-bet. Nature 546, 421–425 (2017). [PubMed: 28607488]
16. Kole A, Maloy KJ, Control of intestinal inflammation by interleukin-10. Curr Top Microbiol Immunol 380, 19–38 (2014). [PubMed: 25004812]
17. Glocker EO et al. , Inflammatory bowel disease and mutations affecting the interleukin-10 receptor. N Engl J Med 361, 2033–2045 (2009). [PubMed: 19890111]
18. Rubtsov YP et al. , Regulatory T cell-derived interleukin-10 limits inflammation at environmental interfaces. Immunity 28, 546–558 (2008). [PubMed: 18387831]
19. Gong S et al. , A gene expression atlas of the central nervous system based on bacterial artificial chromosomes. Nature 425, 917–925 (2003). [PubMed: 14586460]
20. Chevrier S et al. , The BTB-ZF transcription factor Zbtb20 is driven by Irf4 to promote plasma cell differentiation and longevity. J Exp Med 211, 827–840 (2014). [PubMed: 24711583]
21. Wan YY, Flavell RA, Identifying Foxp3-expressing suppressor T cells with a bicistronic reporter. Proc Natl Acad Sci U S A 102, 5126–5131 (2005). [PubMed: 15795373]
22. Kumar P, Bhattacharya P, Prabhakar BS, A comprehensive review on the role of co-signaling receptors and Treg homeostasis in autoimmunity and tumor immunity. J Autoimmun 95, 77–99 (2018). [PubMed: 30174217]
23. Zhang H, Kuchroo V, Epigenetic and transcriptional mechanisms for the regulation of IL-10. Semin Immunol 44, 101324 (2019). [PubMed: 31676122]
24. Kim HJ et al. , Stable inhibitory activity of regulatory T cells requires the transcription factor Helios. Science 350, 334–339 (2015). [PubMed: 26472910]
25. Elkord E, Abd Al Samid M, Chaudhary B, Helios, and not FoxP3, is the marker of activated Tregs expressing GARP/LAP. Oncotarget 6, 20026–20036 (2015). [PubMed: 26343373]
26. Sugimoto N et al. , Foxp3-dependent and -independent molecules specific for CD25+CD4+ natural regulatory T cells revealed by DNA microarray analysis. Int Immunol 18, 1197–1209 (2006). [PubMed: 16772372]

27. Thornton AM et al. , Expression of Helios, an Ikaros transcription factor family member, differentiates thymic-derived from peripherally induced Foxp3+ T regulatory cells. J Immunol 184, 3433–3441 (2010). [PubMed: 20181882]
28. Hamano R, Wu X, Wang Y, Oppenheim JJ, Chen X, Characterization of MT-2 cells as a human regulatory T cell-like cell line. Cell Mol Immunol 12, 780–782 (2015). [PubMed: 25544500]
29. Chen S et al. , Regulatory T cell-like activity of Foxp3+ adult T cell leukemia cells. Int Immunol 18, 269–277 (2006). [PubMed: 16361311]
30. Lee S et al. , Accelerated cell cycle progression of human regulatory T cell-like cell line caused by continuous exposure to asbestos fibers. Int J Oncol 50, 66–74 (2017). [PubMed: 27878235]
31. Chassaing B, Aitken JD, Malleshappa M, Vijay-Kumar M, Dextran sulfate sodium (DSS)-induced colitis in mice. Curr Protoc Immunol 104, Unit 15 25 (2014).
32. Lee PP et al. , A critical role for Dnmt1 and DNA methylation in T cell development, function, and survival. Immunity 15, 763–774 (2001). [PubMed: 11728338]
33. Gavin MA et al. , Foxp3-dependent programme of regulatory T-cell differentiation. Nature 445, 771–775 (2007). [PubMed: 17220874]
34. France MM, Turner JR, The mucosal barrier at a glance. J Cell Sci 130, 307–314 (2017). [PubMed: 28062847]
35. Edelblum KL et al. , The Microbiome Activates CD4 T-cell-mediated Immunity to Compensate for Increased Intestinal Permeability. Cell Mol Gastroenterol Hepatol 4, 285–297 (2017). [PubMed: 28795125]
36. Saraiva M, O'Garra A, The regulation of IL-10 production by immune cells. Nat Rev Immunol 10, 170–181 (2010). [PubMed: 20154735]
37. Lui PP, Cho I, Ali N, Tissue regulatory T cells. Immunology 161, 4–17 (2020). [PubMed: 32463116]
38. Munoz-Rojas AR, Mathis D, Tissue regulatory T cells: regulatory chameleons. Nat Rev Immunol 21, 597–611 (2021). [PubMed: 33772242]
39. Yadav M, Stephan S, Bluestone JA, Peripherally induced tregs - role in immune homeostasis and autoimmunity. Front Immunol 4, 232 (2013). [PubMed: 23966994]
40. Atarashi K et al. , Induction of colonic regulatory T cells by indigenous Clostridium species. Science 331, 337–341 (2011). [PubMed: 21205640]
41. Geuking MB et al. , Intestinal bacterial colonization induces mutualistic regulatory T cell responses. Immunity 34, 794–806 (2011). [PubMed: 21596591]
42. Samanta A et al. , TGF-beta and IL-6 signals modulate chromatin binding and promoter occupancy by acetylated FOXP3. Proc Natl Acad Sci U S A 105, 14023–14027 (2008). [PubMed: 18779564]
43. Owen DL et al. , Thymic regulatory T cells arise via two distinct developmental programs. Nat Immunol 20, 195–205 (2019). [PubMed: 30643267]
44. Weiss JM et al. , Neuropilin 1 is expressed on thymus-derived natural regulatory T cells, but not mucosa-generated induced Foxp3+ T reg cells. J Exp Med 209, 1723–1742, S1721 (2012). [PubMed: 22966001]
45. Campos-Mora M et al. , CD4+Foxp3+T Regulatory Cells Promote Transplantation Tolerance by Modulating Effector CD4+ T Cells in a Neuropilin-1-Dependent Manner. Front Immunol 10, 882 (2019). [PubMed: 31068948]
46. Szurek E et al. , Differences in Expression Level of Helios and Neuropilin-1 Do Not Distinguish Thymus-Derived from Extrathymically-Induced CD4+Foxp3+ Regulatory T Cells. PLoS One 10, e0141161 (2015).
47. Cosovanu C, Neumann C, The Many Functions of Foxp3(+) Regulatory T Cells in the Intestine. Front Immunol 11, 600973 (2020). [PubMed: 33193456]
48. Luu M, Steinhoff U, Visekruna A, Functional heterogeneity of gut-resident regulatory T cells. Clin Transl Immunology 6, e156 (2017). [PubMed: 28983404]
49. Tanoue T, Atarashi K, Honda K, Development and maintenance of intestinal regulatory T cells. Nat Rev Immunol 16, 295–309 (2016). [PubMed: 27087661]
50. Pandiyan P et al. , Microbiome Dependent Regulation of Tregs and Th17 Cells in Mucosa. Front Immunol 10, 426 (2019). [PubMed: 30906299]

51. Jankovic D, Kugler DG, Sher A, IL-10 production by CD4+ effector T cells: a mechanism for self-regulation. Mucosal Immunol 3, 239–246 (2010). [PubMed: 20200511]
52. Trinchieri G, Interleukin-10 production by effector T cells: Th1 cells show self control. J Exp Med 204, 239–243 (2007). [PubMed: 17296790]
53. Barbara G et al. , Inflammatory and Microbiota-Related Regulation of the Intestinal Epithelial Barrier. Front Nutr 8, 718356 (2021). [PubMed: 34589512]
54. Abraham C, Cho JH, Inflammatory bowel disease. N Engl J Med 361, 2066–2078 (2009). [PubMed: 19923578]
55. Piche T et al. , Impaired intestinal barrier integrity in the colon of patients with irritable bowel syndrome: involvement of soluble mediators. Gut 58, 196–201 (2009). [PubMed: 18824556]
56. Sapone A et al. , Divergence of gut permeability and mucosal immune gene expression in two gluten-associated conditions: celiac disease and gluten sensitivity. BMC Med 9, 23 (2011). [PubMed: 21392369]
57. Chanez-Paredes SD, Abtahi S, Kuo WT, Turner JR, Differentiating Between Tight Junction-Dependent and Tight Junction-Independent Intestinal Barrier Loss In Vivo. Methods Mol Biol 2367, 249–271 (2021). [PubMed: 33830456]
58. Chan SS, Kyba M, What is a Master Regulator? J Stem Cell Res Ther 3, (2013).
59. Zhang S et al. , The Transcription Factor PLZF Is Necessary for the Development and Function of Mouse Basophils. J Immunol 203, 1230–1241 (2019). [PubMed: 31366712]
60. Constantinides MG, McDonald BD, Verhoef PA, Bendelac A, A committed precursor to innate lymphoid cells. Nature 508, 397–401 (2014). [PubMed: 24509713]
61. Verhoef PA et al. , Intrinsic functional defects of type 2 innate lymphoid cells impair innate allergic inflammation in promyelocytic leukemia zinc finger (PLZF)-deficient mice. J Allergy Clin Immunol 137, 591–600 e591 (2016). [PubMed: 26602165]
62. Godfrey DI, Koay HF, McCluskey J, Gherardin NA, The biology and functional importance of MAIT cells. Nat Immunol 20, 1110–1128 (2019). [PubMed: 31406380]
63. Liu X et al. , Zinc finger protein ZBTB20 promotes Toll-like receptor-triggered innate immune responses by repressing IkappaBalpha gene transcription. Proc Natl Acad Sci U S A 110, 11097–11102 (2013). [PubMed: 23776228]
64. Sun Y et al. , Zbtb20 Restrains CD8 T Cell Immunometabolism and Restricts Memory Differentiation and Antitumor Immunity. J Immunol 205, 2649–2666 (2020). [PubMed: 32998985]
65. Wang Y, Bhattacharya D, Adjuvant-specific regulation of long-term antibody responses by ZBTB20. J Exp Med 211, 841–856 (2014). [PubMed: 24711582]
66. Bialkowska AB, Ghaleb AM, Nandan MO, Yang VW, Improved Swiss-rolling Technique for Intestinal Tissue Preparation for Immunohistochemical and Immunofluorescent Analyses. J Vis Exp, (2016).
67. Koelink PJ et al. , Development of Reliable, Valid and Responsive Scoring Systems for Endoscopy and Histology in Animal Models for Inflammatory Bowel Disease. J Crohns Colitis 12, 794–803 (2018). [PubMed: 29608662]
68. Kim JJ, Shajib MS, Manocha MM, Khan WI, Investigating intestinal inflammation in DSS-induced model of IBD. J Vis Exp, (2012).
69. Erben U et al. , A guide to histomorphological evaluation of intestinal inflammation in mouse models. Int J Clin Exp Pathol 7, 4557–4576 (2014). [PubMed: 25197329]

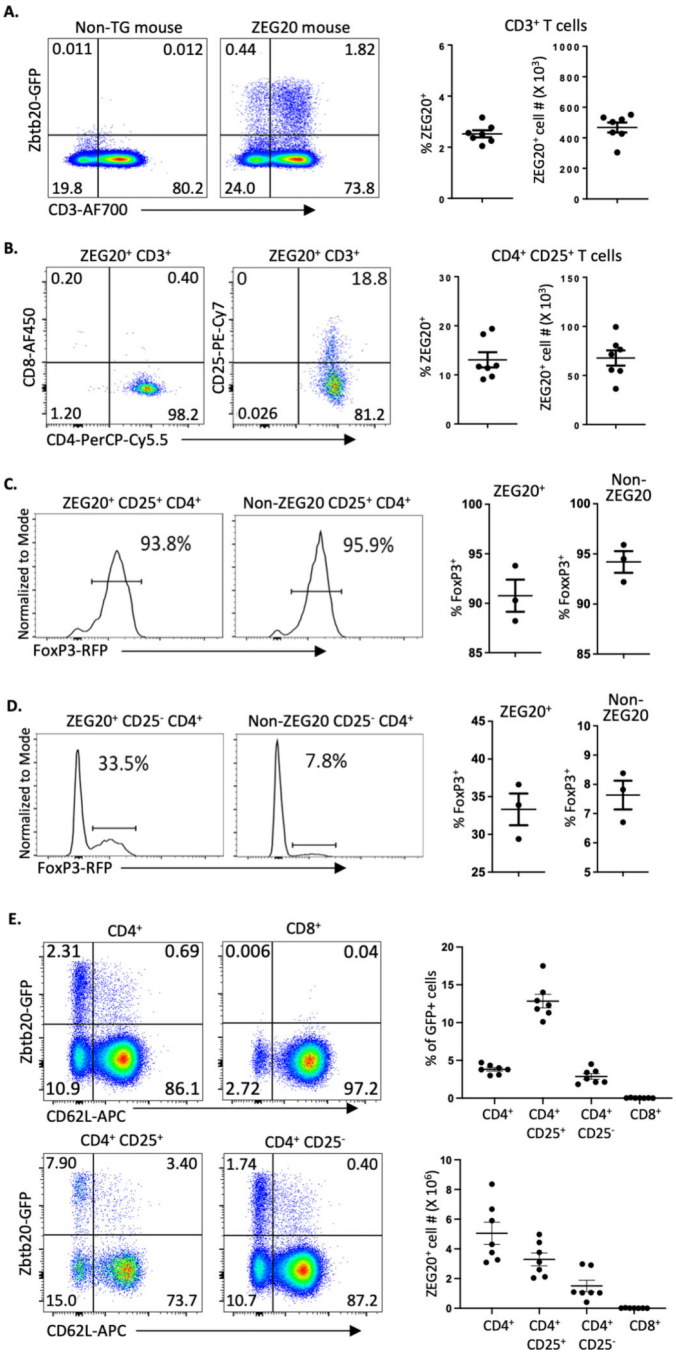


**Figure 1. Zbtb20 expression in T cell subsets**

**(A)** Representative FACS plot and quantification of Zbtb20-GFP$^{+}$ expression in spleen cells from ZEG20 mice (left). A non-transgenic (TG) littermate is shown as a control. Quantification of ZEG20$^{+}$ T cells as a percent of total CD3$^{+}$ T cells and absolute cell numbers (right). (**B**) Representative FACS plot and quantification of CD4 and CD25 expression on ZEG20$^{+}$ T cells (left). Quantification of CD4$^{+}$ CD25$^{+}$ T cells as a percent of total ZEG20$^{+}$ CD4$^{+}$ T cells and absolute cell numbers (right). (**C**) Representative histogram and quantification of FoxP3 expression detected by RFP in ZEG20$^{+}$ CD25$^{+}$ CD4$^{+}$

T cells and non-ZEG20 $CD25^+$ $CD4^+$ T cells and in (**D**) $ZEG20^+$ $CD25^-$ $CD4^+$ T cells and non-ZEG20 $CD25^-$ $CD4^+$ T cells. (**E**) Representative FACS plots and quantification of Zbtb20-$GFP^+$ and CD62L expression in $CD4^+$, $CD8^+$, $CD25^+$ $CD4^+$ and $CD25^-$ $CD4^+$ T cells in spleen of ZEG20 mice. At least two independent experiments were performed. A-B, E n=7 mice/group; C-D n=3 mice/group

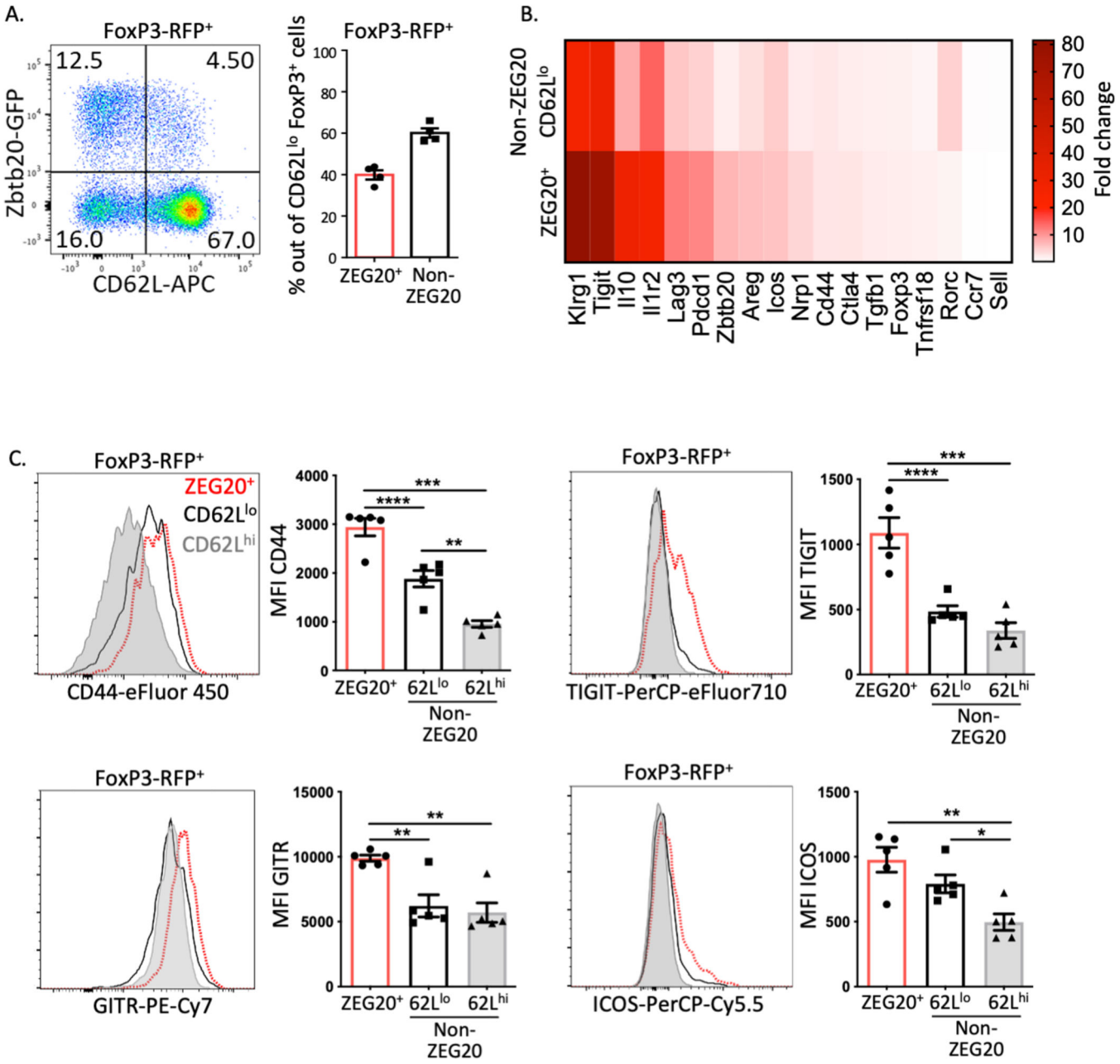


**Figure 2. The phenotype of Zbtb20-expressing Tregs**

(**A**) Representative FACS plot and quantification of CD62L and Zbtb20 expression in Tregs from the spleen of ZEG20;FoxP3-RFP mice. Percent of the ZEG20$^{+}$ and non-ZEG20 populations among CD62L$^{lo}$ Tregs is shown in the graph. (**B**) Heat map of RNA-Seq data represented as the fold-change difference in gene expression in ZEG20$^{+}$ Tregs vs non-ZEG20 CD62L$^{hi}$ Tregs or non-ZEG20 CD62L$^{lo}$ Tregs vs non-ZEG20 CD62L$^{hi}$ Tregs collected from spleens of ZEG20;FoxP3-RFP mice (n=4 mice/group). The heat map shows genes associated with Treg function. (**C**) Representative FACS histograms of CD44, TIGIT, GITR and ICOS expression in ZEG20$^{+}$ or non-ZEG20 CD62$^{lo}$ or non-ZEG20 CD62$^{hi}$ FoxP3$^{+}$ Tregs. Mean fluorescent intensity (MFI) is quantified in graphs. At least three

independent experiments were performed. A-B n=4 mice/group; C n=5 mice/group. Data were analyzed using unpaired One-way ANOVA with Tukey correction and represented as mean ± SEM. Significance represents * P<0.05, ** P<0.01, *** P<0.001

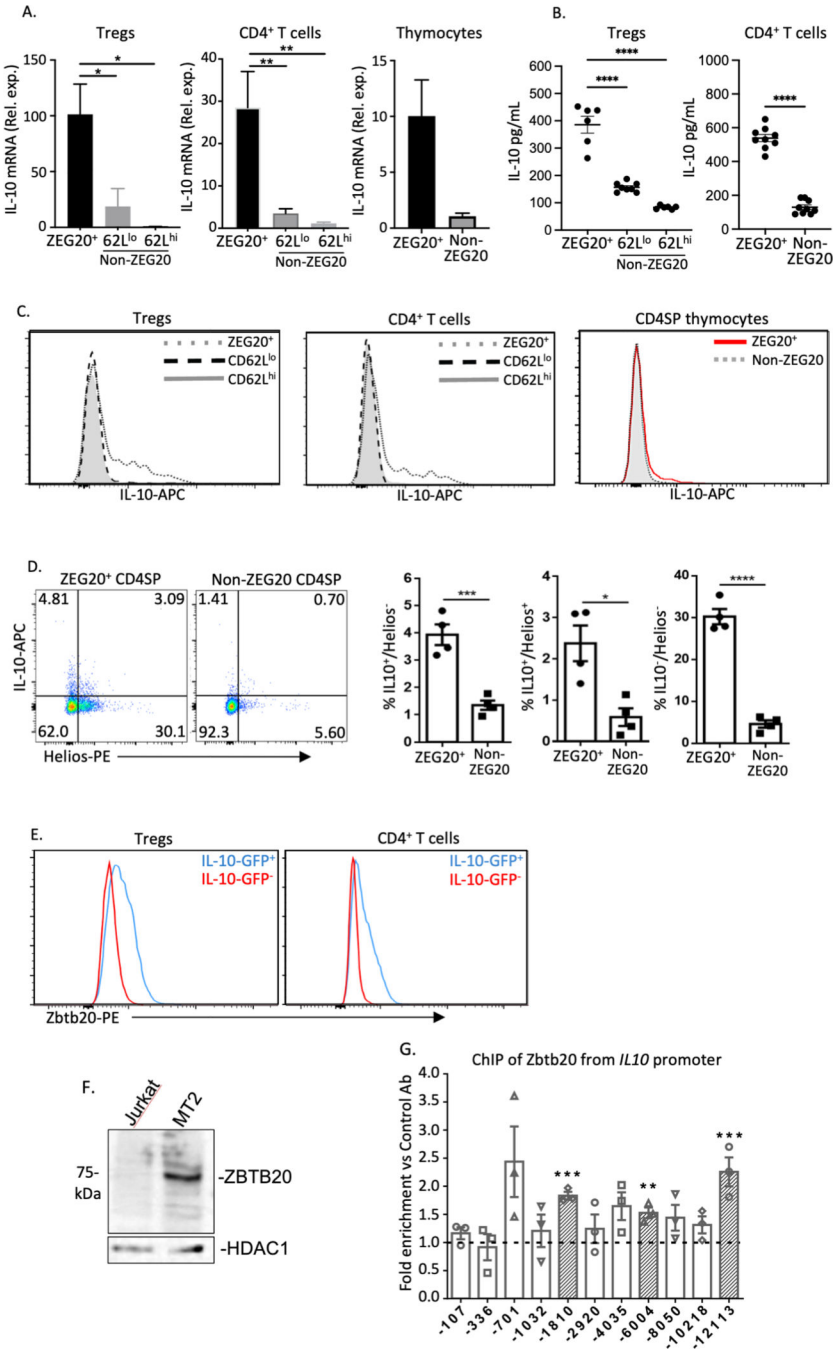


**Fig. 3. Zbtb20-expressing T cells constitutively express *Il10***

*Il10* mRNA level measured by qPCR in the indicated subsets of (**A**) spleen Tregs, CD4$^+$ T cells and thymocytes. (**B** IL-10 released into the medium by the indicated FACS sorted cell subsets 24h post-PMA/ion activation measured with CBA. (**C**) Representative FACS histogram showing IL-10 production by the indicated cell subsets detected by cell surface capture reagent 3h post-PMA/ion activation. (**D**) Representative FACS dot plot and quantification of IL-10 and Helios expression in ZEG20$^+$ and non-ZEG20 thymocytes (left). IL-10 is detected by cell surface capture reagent 3h post-PMA/ion activation. Percent of

the IL-10 and Helios expressing populations among ZEG20$^{+}$ and non-ZEG20 thymocytes is shown in the graph (right). (**E**) ) Representative FACS histogram of Zbtb20 protein expression in IL-10-GFP$^{+}$ and IL-10 GFP$^{-}$ Tregs and CD4$^{+}$ T cells sorted from spleens of IL-10$^{ires\text{-}GFP}$ mice. Cells were permeabilized and stained with anti-Zbtb20-PE antibody (**F**) Zbtb20 expression in MT-2 cells assessed by Western blot. (**G**) ChIP of Zbtb20 bound to the IL10 promoter in MT-2 cells. The X-axis indicates 11 regions identified in the ENCODE database as accessible to transcription factor binding (the indicated base pair number is the position of the 5' primer used for PCR, Table 1), the Y-axis shows the fold enrichment at each site as compared to an IP with an irrelevant antibody (the dotted line). The shaded bars indicate regions with significantly enriched binding of Zbtb20, based on three independent ChIP experiments. For FACS, qPCR and IL-10 release at least three independent experiments were performed. A,C,E total n=3 mice/group; B total n=5–11 mice/group; D total n=4 mice/group. Data were analyzed using an unpaired t-test (D) or One-way ANOVA with Tukey correction (A,B,G) and represented as mean ± SEM. Significance represents * P<0.05, ** P<0.01, *** P<0.001.

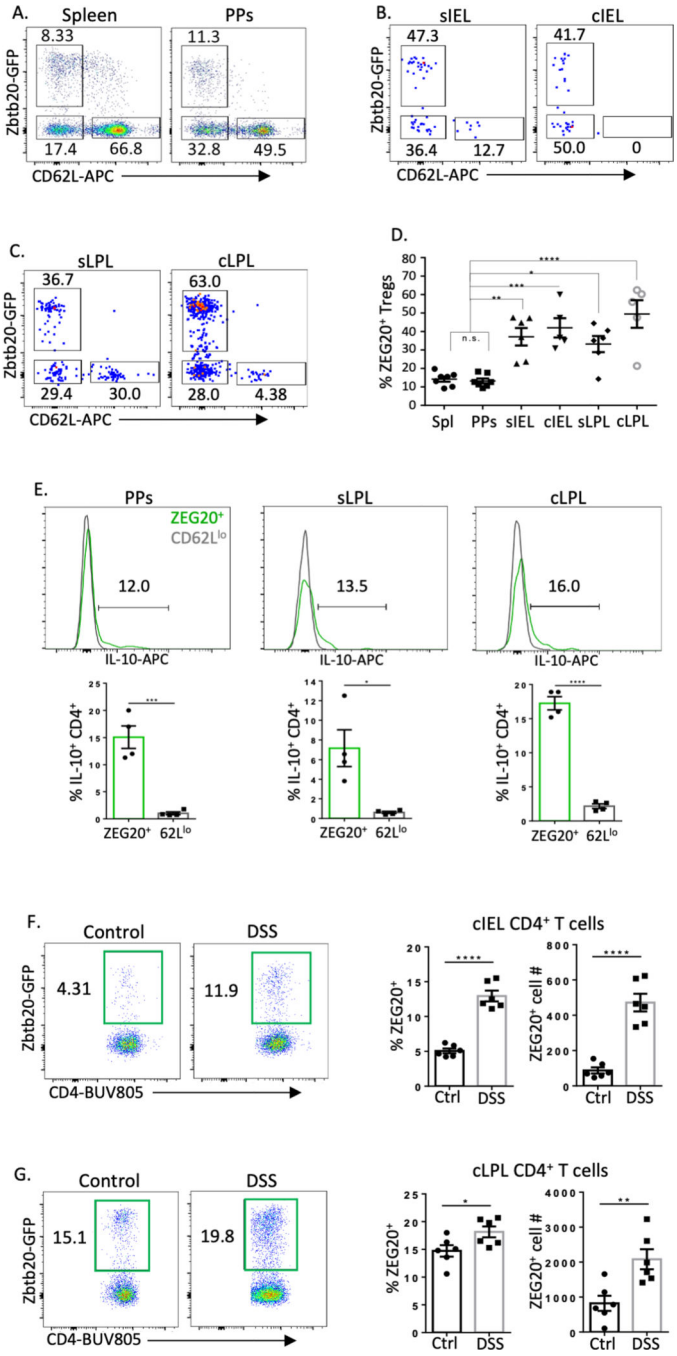


**Fig. 4. Zbtb20-expressing Tregs enriched in the gastrointestinal tract**

(**A**) Representative FACS plot of Zbtb20 and CD62L expression in Tregs from spleens and Peyer's Patches (PP), (**B**) epithelium of the small intestine (sIEL) and colon (cIEL), and (**C**) LP of the small intestine (sLPL) and colon (cLPL). (**D**) Quantification of ZEG20$^+$ Tregs shown in A-C and presented as percentage of ZEG20$^+$ cells among Tregs. (**E**) Representative FACS histogram of IL-10 expression by the indicated subsets detected with cell surface capture reagent after 3h activation with PMA/ion. (**F**) Representative FACS plots and quantification of the increase in ZEG20$^+$ CD4$^+$ T cells in colon epithelium and (**G**) LP

in ZEG20;FoxP3-RFP mice following the DSS treatment. Three independent experiments were performed. A,B,C,D total n=5–7 mice/group; E total n=4 mice/group; F,G total n=6 mice/group. Data were analyzed using an unpaired t-test (E,F,G) or One-way ANOVA with Tukey correction (D) and represented as mean ± SEM. Significance represents * $P<0.05$, ** $P<0.01$, *** $P<0.001$.

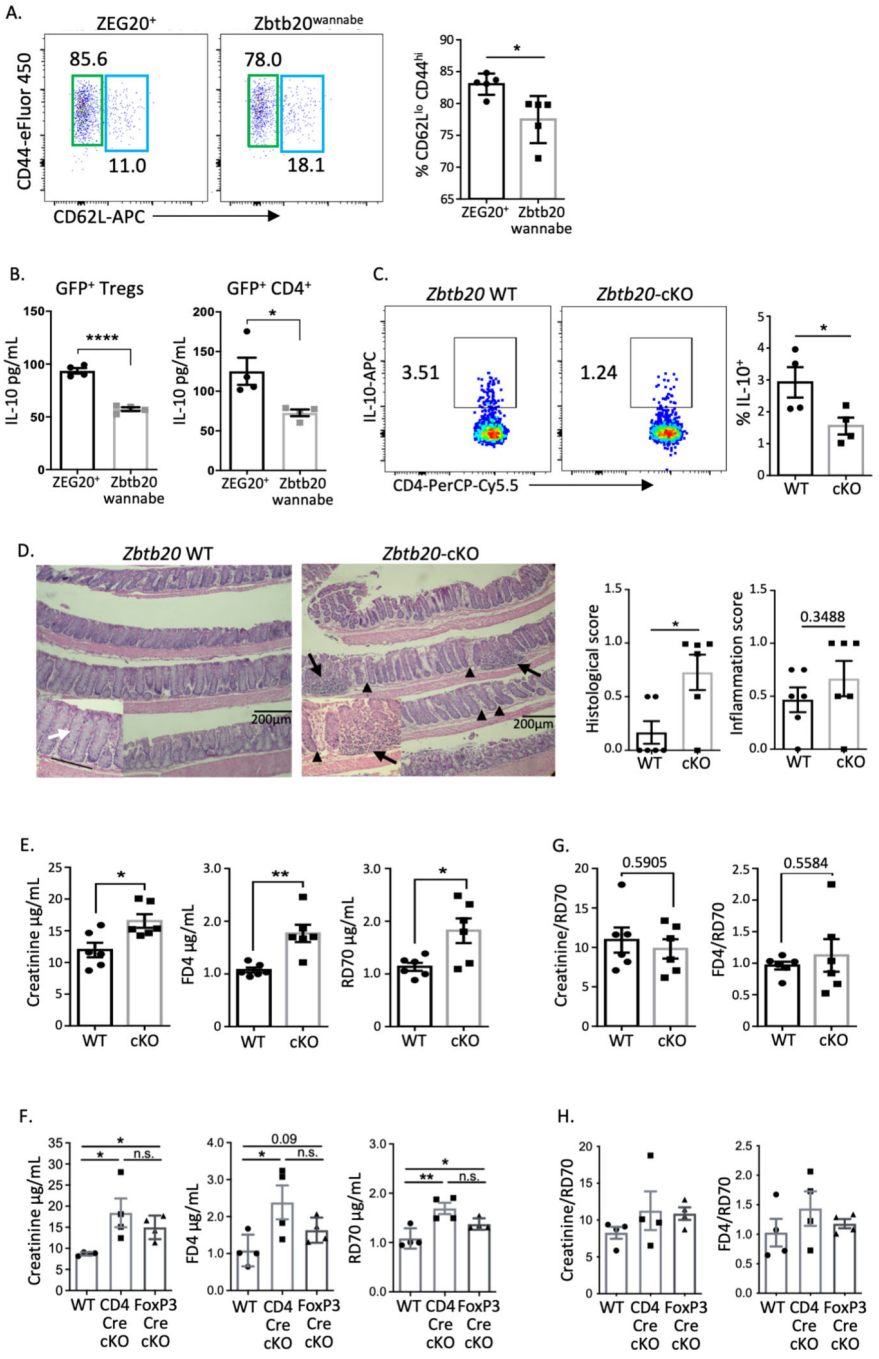


**Fig. 5. *Zbtb20* deletion impacts T cell function and compromises intestinal integrity**

(**A**) Representative FACS plots of CD62L and CD44 expression in ZEG20$^{+}$ and Zbtb20$^{wannabe}$ Tregs from spleens. (**B**) IL-10 released into the medium by sorted ZEG20$^{+}$ and Zbtb20$^{wannabe}$ T cells 24h post PMA/ion activation and measured with CBA. (**C**) Representative FACS plots of IL-10 expression by Tregs from *Zbtb20*$^{fl/fl}$ (WT) and *Zbtb20*-cKO (cKO) mice detected by cell surface capture reagent 3h post-PMA/ion activation. (**D**) Representative sections of colons stained with H&E (left). The histological and inflammation scores reported by blinded analysis of sections done by an uninvolved

third party (right). Images at 10x (scale bar = 200μm) and 40x (insert) magnification. Lymphocytic nodules indicated by arrows, and areas of mild crypt hyperplasia and mucosal edema are shown by arrowheads. The black line and white arrow in the insert of WT show abundant goblet cells. (**E, F**) The concentration of creatinine, FITC-dextran (FD4), and rhodamine B-dextran (RD70) in the serum of 14-week old WT, cKO (CD4-Cre;Zbtb20$^{fl/fl}$) and (**F**) FoxP3-Cre;Zbtb20$^{fl/fl}$ mice 5h after gavage. (**G, H**) Ratios of creatinine to rhodamine B-dextran (Creatinine/RD70) and FITC-dextran to rhodamine B-dextran (FD4/RD70). At least two independent experiments were performed. A total n=5 mice/group; B,C total n=4 mice/group; D,E,G total n=6 mice/group; F,H total n=4 mice/group. Data were analyzed using an unpaired t-test and represented as mean ± SEM. Significance represents * P<0.05, ** P<0.01, *** P<0.001.

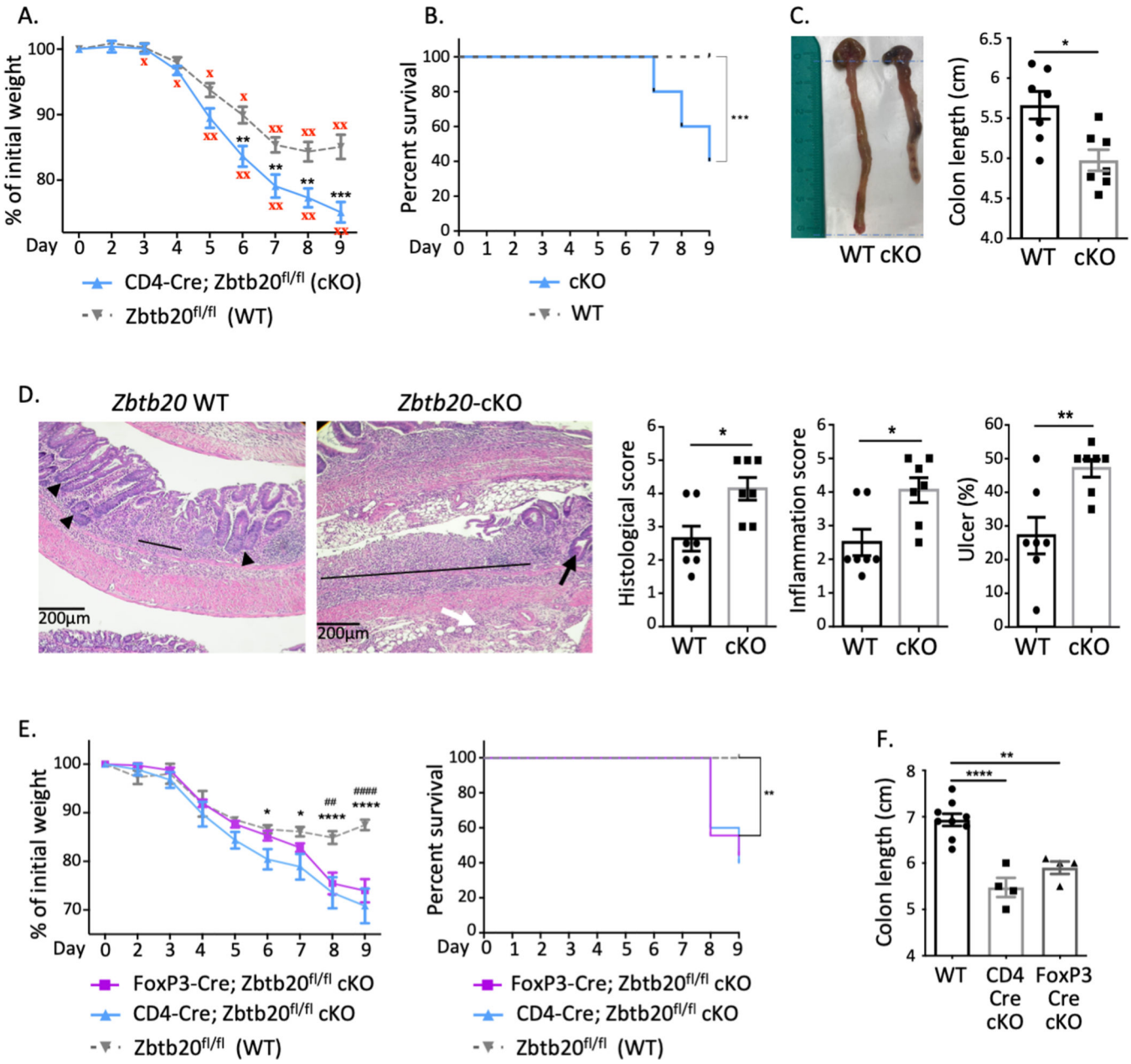


**Fig. 6. *Zbtb20*-cKO mice develop severe colitis**

(**A**) Bodyweight and (**B**) survival of Zbtb20$^{fl/fl}$ (WT) and *Zbtb20*-cKO (cKO) mice with DSS-induced colitis; * indicates significance, the single red x indicates the presence of occult blood in the stool, the double red x indicates the presence of visible blood. (**C**) Representative image and measurements of the lengths of the colons from WT and cKO mice with DSS-induced colitis. (**D**) Representative H&E stained sections of colons collected from 8-week old WT and cKO mice collected 9 days after initiation of DSS treatment (left). Ulcerated regions indicated by underlying lines (focal in WT and extensive in cKO); atypical crypt hyperplasia in WT (arrowhead) and cKO with crypt dilatation (black arrow); inflammatory infiltrate (white arrow). Histological and inflammation scores and size of the ulcer were reported by blinded analysis of sections done by an uninvolved third party;

(right); 10x magnification (scale bar = 200μm). (**E**) Bodyweight and survival of WT, CD4-Cre;cKO, and FoxP3-Cre;cKO mice following induction of colitis. (* indicates significance between CD4-Cre;cKO and WT; # indicates significance between FoxP3-Cre;cKO and WT. (**F**) The lengths of the colons in the mice with DSS-induced colitis. A,B,E n=10–14 mice mice/group; C,D n=7 mice/group; F,G total n=4–9 mice/group. Data were analyzed using an unpaired t-test and represented as mean ± SEM. Significance represents * P<0.05, ** P<0.01, *** P<0.001.

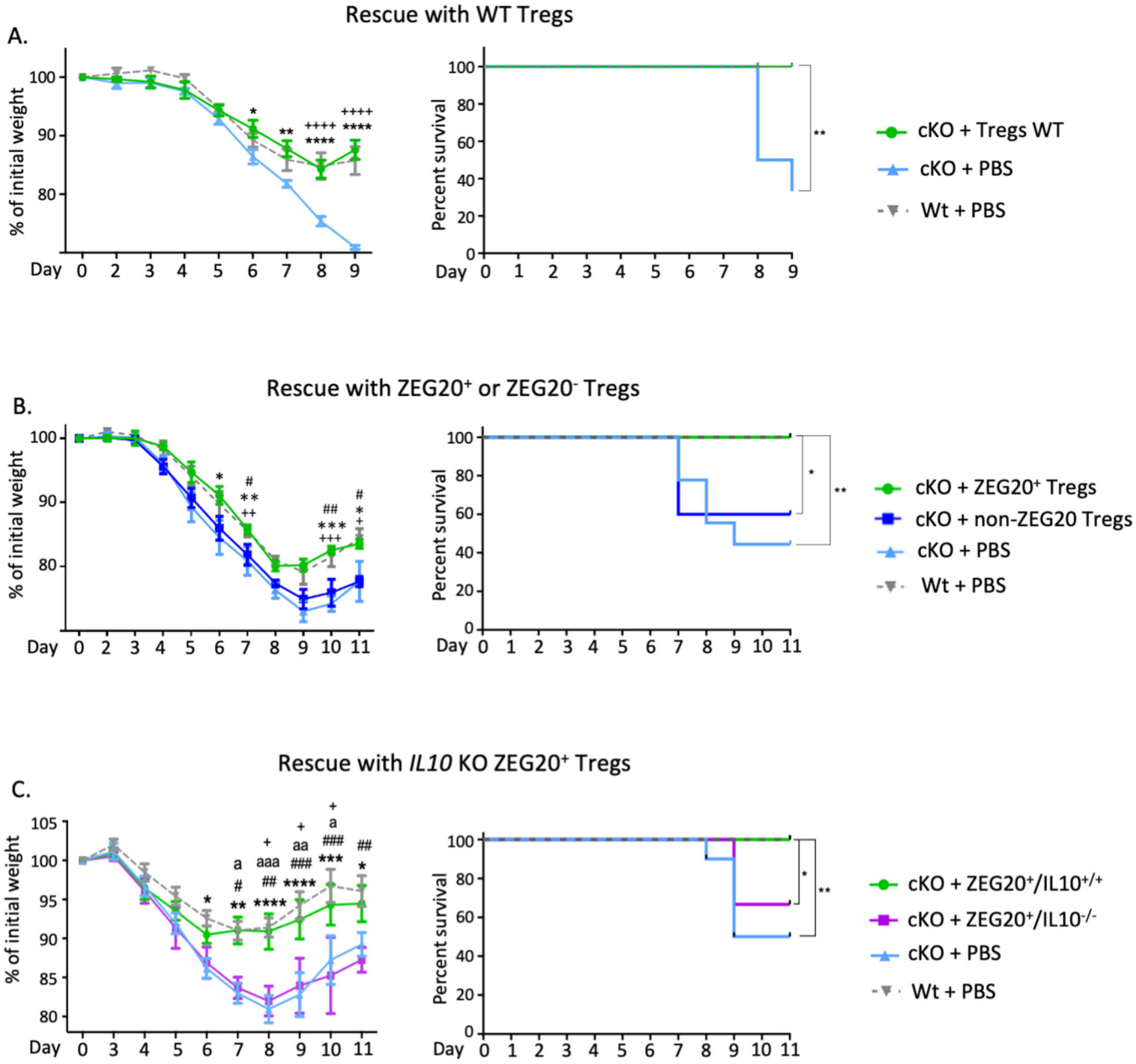


**Fig. 7. Adoptive transfer of Zbtb20-expressing Tregs reduces the severity of colitis.**

(A) Bodyweight and survival of WT and *Zbtb20*-cKO (cKO) mice that received an i.p. injection of the vehicle (PBS) or $5\times10^5$ of total Tregs collected from the spleen of healthy WT mouse (* indicates significance between WT + PBS and cKO + PBS; $^+$ indicates significance between cKO + Tregs WT and cKO + PBS). (**B**) Bodyweight and survival of WT and cKO mice that received an i.p. injection of PBS or $100\times10^3$ sorted ZEG20$^+$ Tregs or $1\times10^5$ sorted non-ZEG20 CD62L$^{lo}$ Tregs ($^\#$ indicates significance between cKO + ZEG20$^+$ and cKO + non-ZEG20 CD62L$^{lo}$; * indicates significance between cKO + ZEG20$^+$ and cKO + PBS; $^+$ indicates WT + PBS and cKO + PBS). (**C**) Bodyweight and survival of WT and cKO mice that received an i.p. injection of PBS or $100\times10^3$ sorted ZEG20$^+$ IL-10$^{+/+}$ Tregs or $1\times10^5$ sorted ZEG20$^+$ IL-10$^{-/-}$ Tregs ($^a$ indicates significance between

cKO + ZEG20$^{+}$ Tregs and cKO + PBS; $^{+}$ indicates significance between cKO + ZEG20$^{+}$ Tregs and cKO + ZEG20 IL-10$^{-/-}$ Tregs; $^{\#}$ indicates significance between WT + PBS and cKO + ZEG20 IL-10$^{-/-}$ Tregs ; * indicates significance between WT + PBS and cKO + PBS). The injections were done a day before induction of the colitis with DSS. At least two independent experiments were performed. A total of n=6 mice/group. B total n=5–9 mice/group. C total n=6–9 mice/group. Data were analyzed using two-way ANOVA with Tukey correction and represented as mean ± SEM. Significance represents * P<0.05, ** P<0.01, *** P<0.001.

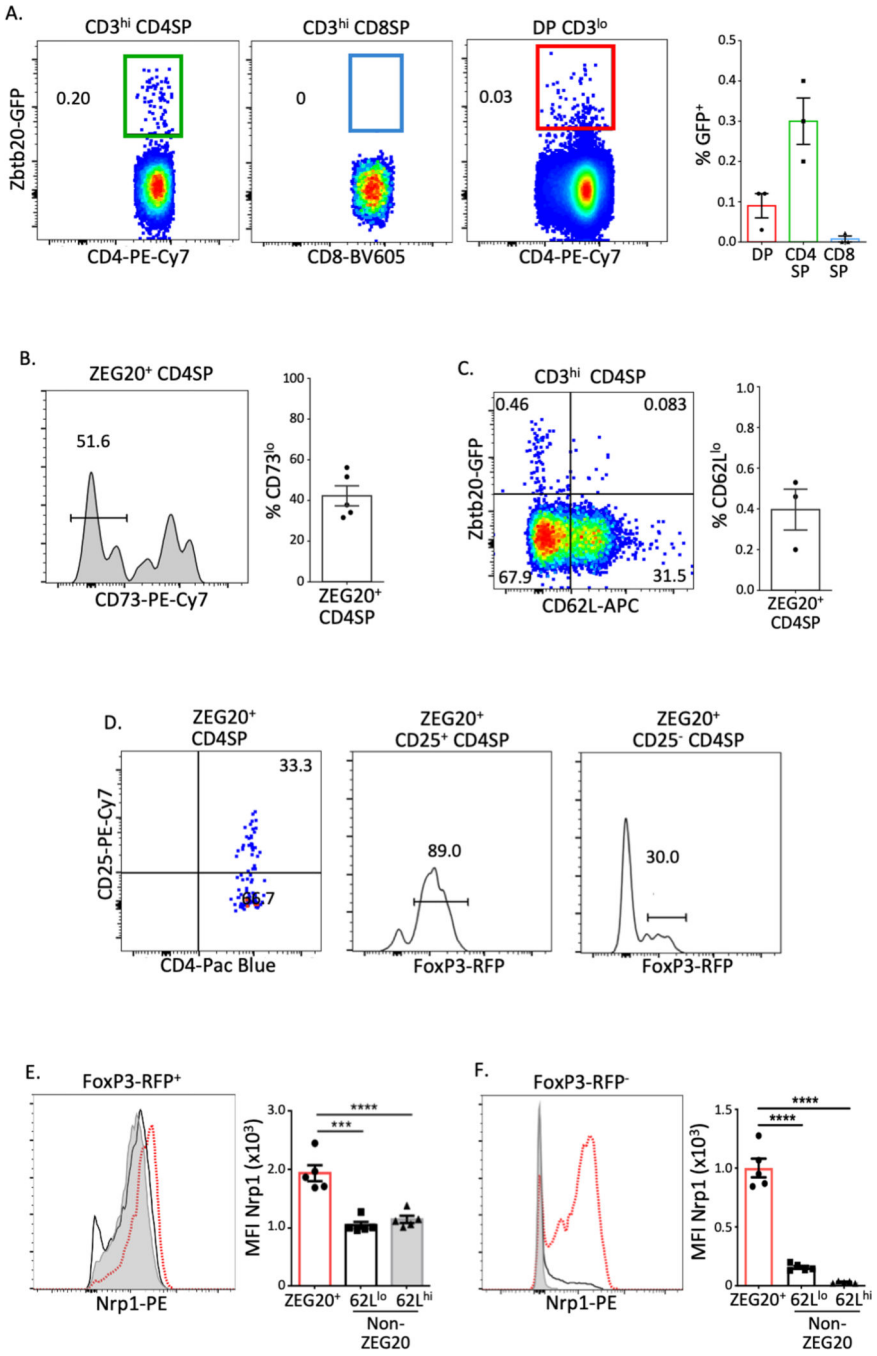


**Fig. 8. Zbtb20 expression during thymic development**

(**A**) Representative FACS dot plot of Zbtb20 expression in CD3$^{hi}$CD4SP and CD3$^{hi}$CD8SP and CD3$^{lo}$DP thymocytes in ZEG20 mice. (**B**) Representative FACS plots showing expression of CD73, (**C**) CD62L, (**D**) CD25, and FoxP3 in ZEG20$^{+}$ CD4SP thymocytes. (**E**) Representative FACS histogram of Nrp-1 expression in the indicated subsets of Tregs and (**F**) T cells from spleens of ZEG20;FoxP3-RFP mice. At least two independent experiments were performed. A,C,D total n=3 mice/group. B,E,F total n=5 mice/group. Data were

analyzed using One-way ANOVA and represented as mean ± SEM. Significance represents * P<0.05, ** P<0.01, *** P<0.001.

**Table 1.**

Primers used for PCR

| Primers | Forward (5’−3’) | Reverse (5’−3’) |
|---|---|---|
| Exon 13 | CTAGAACGGAAGAAACCCAAGAA | |
| Exon 14 | CTGACCTTGACCAGCAACACACG | AGCAAATGGAGCGCTACCTGTCCA |
| Exon 15 | | GGATTACCTTATCAAGCACATGGTGAC |
| hIL10_−107 | GGAGGAGCTCTAAGCAGAA | AAGCCCCTGATGTGTAGAC |
| hIL10_−336 | CTAGGAACACGCGAATGAGAA | TTTAGGATGGGCTACCTCTCT |
| hIL10_−701 | GCAGACTACTCTTACCCACTTC | TGTGTTCCAGGCTCCTTTAC |
| hIL10_−1032 | GAGGAAAGTAAGGGACCTCCTA | CTTCTGTGGCTGGAGTCTAAAG |
| hIL10_−1810 | AGTTTCTAGCAGGCTCTTTCTC | GGTGTCTCTTCCCAACTCTTC |
| hIL10_−2920 | CTTCAGCAAATGGCTTGAGATAAT | TGCTGAGATTACAGGCATGAG |
| hIL10_−4035 | GCTCTAATGGGAGGCAGATT | GTGTGTGTGTGTGTGCTTATG |
| hIL10_−6004 | GTGGAGACTGGAGCAAACTAA | GTCTGCATGACTACCTAGGATAAC |
| hIL10_−8050 | CGCCTGGAAGAGCACTAAT | TGAAGAAACCACTGTCCTTACA |
| hIL10_−10218 | GACAGGTCACTGGCAAATCA | CCAGGGTGGTCTTTCAGTTTAG |
| hIL10_−12113 | TCTTCTGATTTCCACTGCTCTC | TGTATTTCCTTCTCGCAATCCT |